FINAL REPORT

JPL Contract 954 563

Winston Solar Concentrators and Evaluation Support

Phase II. Non-Imaging Concentrators for Space Applications

Principal Investigator: Professor Roland Winston

Co Investigator: Dr. Joseph O'Gallagher

Research Assistant: Peretz Greenman

Period Covered: October 1977 - July 1978

Date Submitted: August 28, 1978

THE ENRICO FERMI INSTITUTE

THE UNIVERSITY OF CHICAGO

JPL Contract 954 563

Winston Solar Concentrators and Evaluation Support

Phase II. Non-Imaging Concentrators for Space Applications

FINAL REPORT

Principal Investigator: Professor Roland Winston

Co Investigator: Dr. Joseph O'Gallagher

Research Assistant: Peretz Greenman

Period Covered: October 1977 - July 1978

Date Submitted: August 28, 1978

Work Performed by:

The University of Chicago
Enrico Fermi Institute
5630 S. Ellis Avenue
Chicago, Illinois 60637

ABSTRACT

A detailed analytical and experimental study of a 4.67 X, $\pm 5^{\circ}$ Compound Parabolic Concentrator (CPC) for a large photovoltaic array in space has been completed. The design has been demonstrated to be effective in achieving a net power gain which can be varied from more than a factor of 3 down to approximately unity. A method for reducing non-uniformities in illumination to a given desired level has been found. The effectiveness of this method, which involves the introduction of a degree of non-specularity in the reflector surface, has been confirmed by direct measurements with prepared foil reflectors in a CPC in terrestial sunshine as well as by detailed computer ray tracing. Further ray tracing confirms that the CPC design is extremely tolerant to pointing and alignment errors, minor distortions etc. Furthermore a two stage non-imaging design has been shown by preliminary measurements and analysis to provide both the desired angular tolerance and the required degree of intensity uniformity if higher concentrations (4X-10X) are necessary.

Table of Contents

LIST OF TABLES

LIST OF FIGURES

I. Introduction

A. Background

This contract was initiated in July of 1976 with the initial objective of conducting a feasibility study regarding the use of the Compound Parabolic Concentrator (CPC) with photovoltaic arrays in space applications. Phase I of the study consisted in: a) the design, fabrication and testing of selected CPC specimen concentrators in conjunction with small (single cell wide) solar arrays; b) design of a model for a representative baseline CPC configuration for a large concentrator-array combination; and c) preliminary analytical studies regarding the behavior and possible reduction of non-uniformities in the intensity distribution of concentrated solar radiation on the solar cell surface. These activities covered the period from July 1976 - September 1977 and are described in greater detail in the Phase I Final Report submitted March 1978.[1)] Phase II commenced formally in February 1978 and was directed towards a detailed study of the baseline configuration and the problem of nonuniformity. The formal technical contract requirements were completed in June 1978 and an oral presentation of the results of the work was given on July 20 at JPL. This document summarizes the techical results of the Phase II activities.

B. Highlights

The major accomplishments of the project effort are summarized below:

1) CPC's have been demonstrated to be very effective in achieving power gains in the range of a factor of 3 to 4 with reflector height to aperture ratios ~ 1.

2) A method for reducing the degree of non-uniformity in the intensity distribution to a desired level while at the same time minimizing the associated optical losses has been developed analytically and confirmed experimentally. The method involves the use of reflectors with a controlled degree of non-specularity in the reflector surface.

3) A simple method for varying the effective geometrical concentration to cover the range from ~ 1.5 to ~ 5 has been developed and tested.

4) Extensive ray trace analyses have been carried out which confirm that the selected concentrator baseline design is extremely tolerant of pointing and alignment errors, mirror distortions, reflector placement and spacing, etc.

5) Optical models and computer codes have been developed which are capable of analyzing a wide range of concentrator designs.

6) A preliminary study of two-stage non-imaging concentrator designs indicates that such configurations are quite effective if higher concentration ratios (5x - 10x) are desired.

C. Project Review

During Phase I, the staff at the University designed, built, tested and delivered to JPL four specimen concentrators. The optical performance of the concentrators and electrical performance of the cells with and without concentrators was measured. The results were in precise agreement with model predictions and showed that effective gains in the

maximum power and short circuit current in the range of 70% to 80% of the geometrical concentration ratio (i.e., ~ 3.5 for a 4.75 x concentrator) were readily achievable. The major problem area identified was that for large arrays utilizing many cells at the exit aperture of a single large concentrator, positional intensity variations might limit effective gain of the array. A preliminary solution to this problem involving the introduction of small angle scattering in the reflector surface was proposed and a CPC having a geometrical concentration ratio of 4.67x and an acceptance half angle of $\pm 5^{o}$ was selected for more detailed study. For further details see Reference 1.

This report is concerned mainly with the activities carried out in Phase II. The major milestones of this effort were to;

1) Complete detailed computer ray trace analysis of the baseline configuration.

2) Analytically predict the effectiveness of the non-specular method for reducing non-uniformities and determined quantitatively the desired degree of non-specularity to achieve a given reduction.

3) Participate with JPL staff in a test of a scale model concentrator with variable geometric concentration at the General Electric facility in Valley Forge, Pennsylvania.

4) Fabricate at Chicago a scale model of the baseline configuration with the capability of interchanging reflecting foil surfaces.

5) Carry out experimental measurements at the University in terrestrial sunshine to confirm the ray-trace predictions of

a substantial reduction in non-uniformities.

6) Carry out further analytical studies of concentrator tolerances for induced distortions and reflector spacing variations.

7) Measure optical characteristics of sample reflector materials.

8) Carry out an analysis of selected alternate optical approaches using a CPC baseline for concentration in space.

A detailed discussion of the above milestones, preceeded by a short review of the principles and features of Compound Parabolic Concentrators forms the body of the remainder of the report.

II. Compound Parabolic Concentrators for Space Application

A. General Principles and Features of CPC's

CPC's are one type of a newly discoverd class of optical devices, referred to as "ideal" light collectors, which achieve the maximum concentration permitted by the laws of physics for any view angle. The basic features were discovered independently at essentially the same time in the USA, (R. Winston, 1966), the Soviet Union, (Baranov, 1966) and Germany (Ploke, 1966). Most of the development of the optical concept has taken place in the United States at either Argonne National Laboratory or the University of Chicago under the direction of Professor Winston.

The simplest form of a CPC is that which concentrates light onto a flat absorber and is therefore the shape of interest for combination with a flat solar array. This type of CPC is a cone of revolution or longitudinaly extended trough whose cross sectional profile is shown in Figure 1. It consists of two parabolic segments, each positioned so that its focus is at the lower edge of its symmetric counterpart and tilted by an angle $\pm\theta_c$ with respect to the optic axis. It acts like a light funnel in that all rays incident on the entrance aperture A, at angles $\theta \leq \theta_c$ will (after 0, 1, 2 or more reflections) strike the exit apertures A_2. The geometric concentration ratio for the 2 dimensional trough is

$$C_{max} = A_1/A_2 = \frac{1}{\sin\theta_c} \tag{1}$$

for a "full height" CPC with height

$$h_{max} = \frac{A_1+A_2}{2} \operatorname{ctn} \theta_c \tag{2}$$

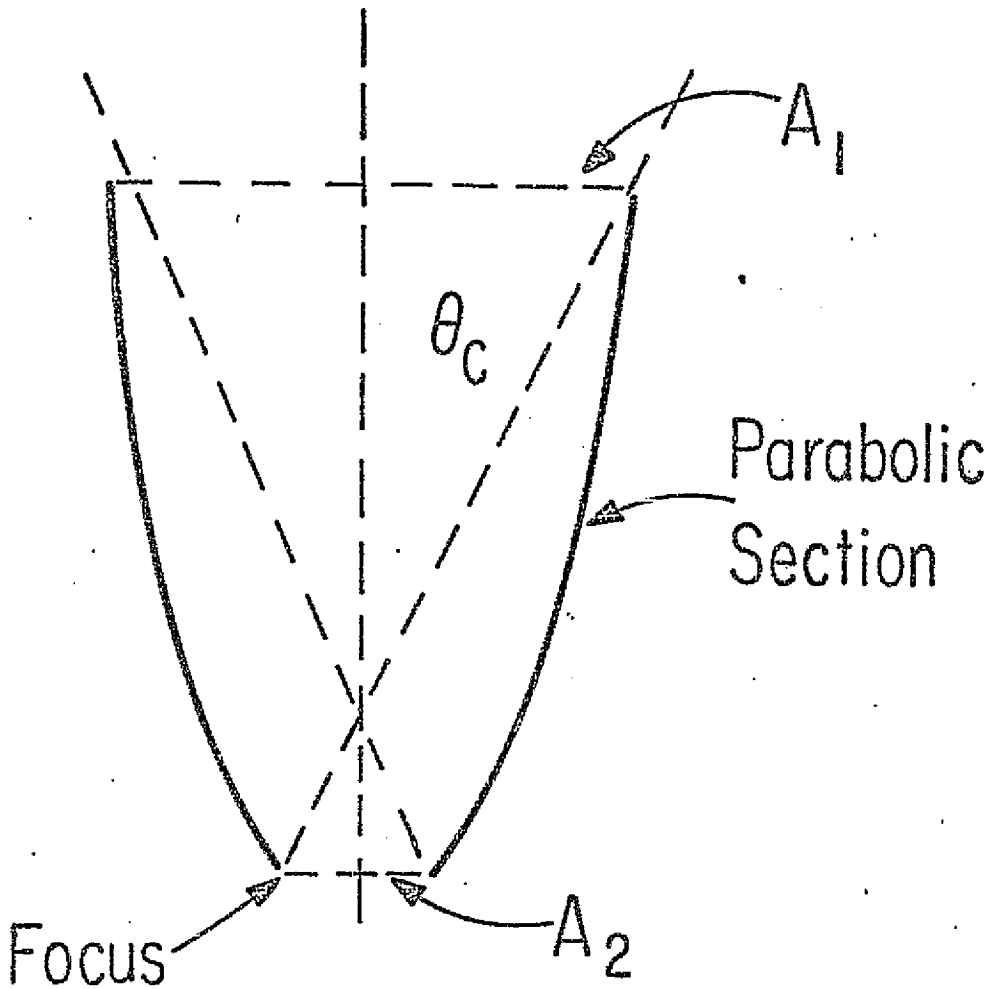

Features:

1) Is an "IDEAL" Conc.
2) Accepts all rays with $\theta < \theta_c$
3) Rejects all rays with $\theta > \theta_c$
4) Has $C = A_1/A_2 = 1/\sin\theta_c$
$= C_{max}$

FIGURE 1 COMPOUND PARABOLIC CONCENTRATOR FEATURES

obtained by extending the parabolic to the dotted lines at angles $\pm\theta_c$ from the edges of A_2. Most CPC's are "truncated" (cut down) to only fractions of their full height, thus saving substantially on height to aperture ratio and reflector area but resulting in concentration ratios less than C_{max} for a given θ_c. The relationship between degree of truncation, acceptance angle and C_{geom} is given in Figure 2 taken from a paper by Rabl (1967).[2] The fundamental advantage of a CPC is its wide view angle resulting in greatly improved tolerances to mirror slope and alignment errors, pointing errors, tracking requirements, etc.

The effect achieved by combining a CPC with a solar cell is illustrated in Figure 3 which shows the I-V curve for an array of 3 cells (each 4 cm x 2 cm) long and one cell wide for a) no concentration, b) a CPC with $C_{geom} = 2.93$, and c) a CPC with $C_{geom} = 4.75$. The average optical efficiency as measured by the gain in short circuit current is 0.82 but varies somewhat due to differences in atmospheric conditions on different days. (The CPC performance is worse on hazy days because it sees only a fraction of the diffuse component which of course is irrelevant for space applications). The fill factor degrades slightly under concentration due to the increased equilibrium cell temperatures and the resulting drop in open circuit voltage. Other effects of concentration are non-uniformities in the intensity distribution on the cell surface to be discussed in detail in subsequent sections and a reduction in the effective view angle of the cell. That is, the bare cell sees effectively one hemisphere while the concentrator limits incidence to a "wedge" of angles centered on the optic axis. The angular response of a $\pm 5^{\circ}$ CPC truncated to 4.75 X as measured by cell

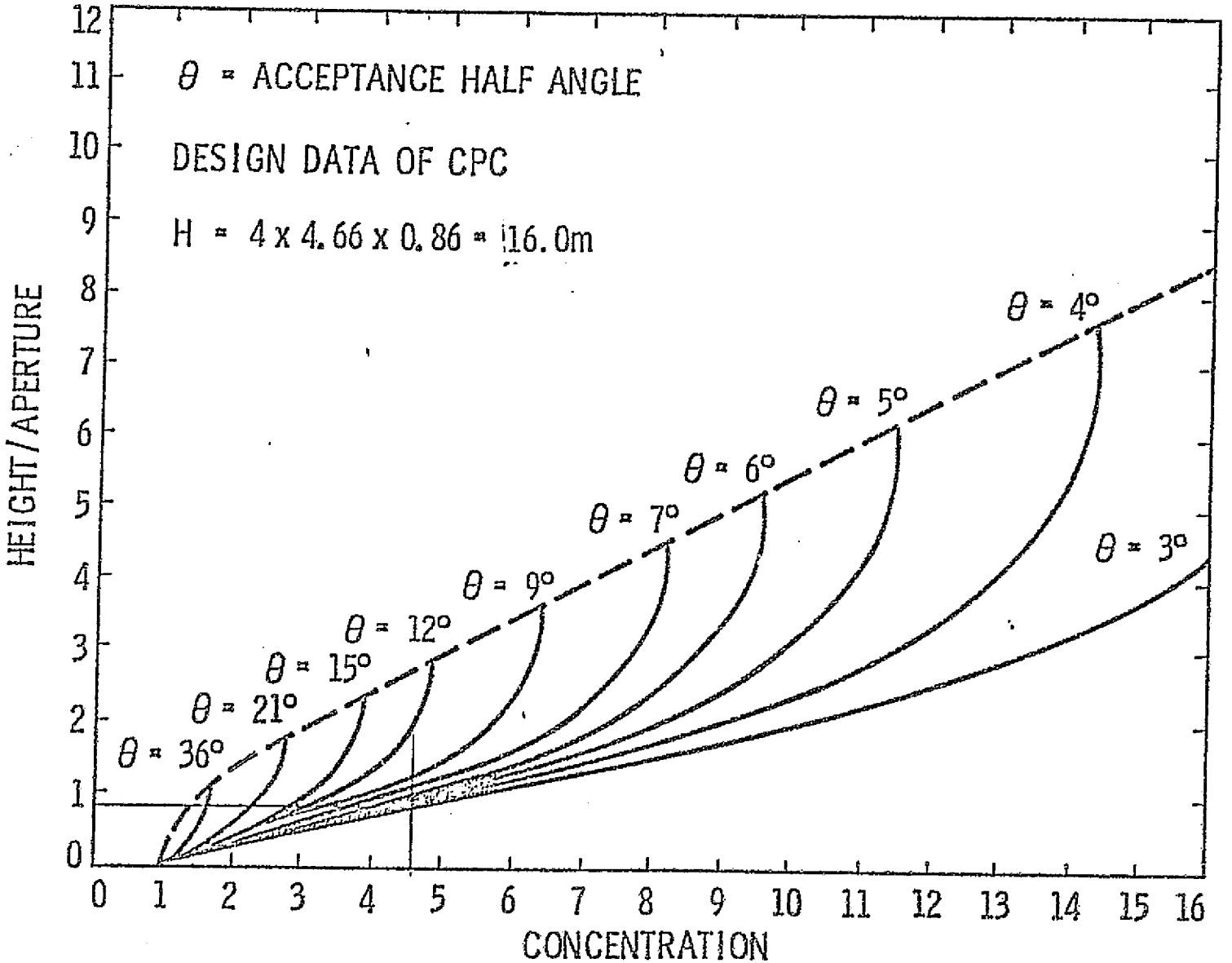

FIGURE 2

HEIGHT/APERTURE RATIO FOR FULL AND FOR TRUNCATED CPC

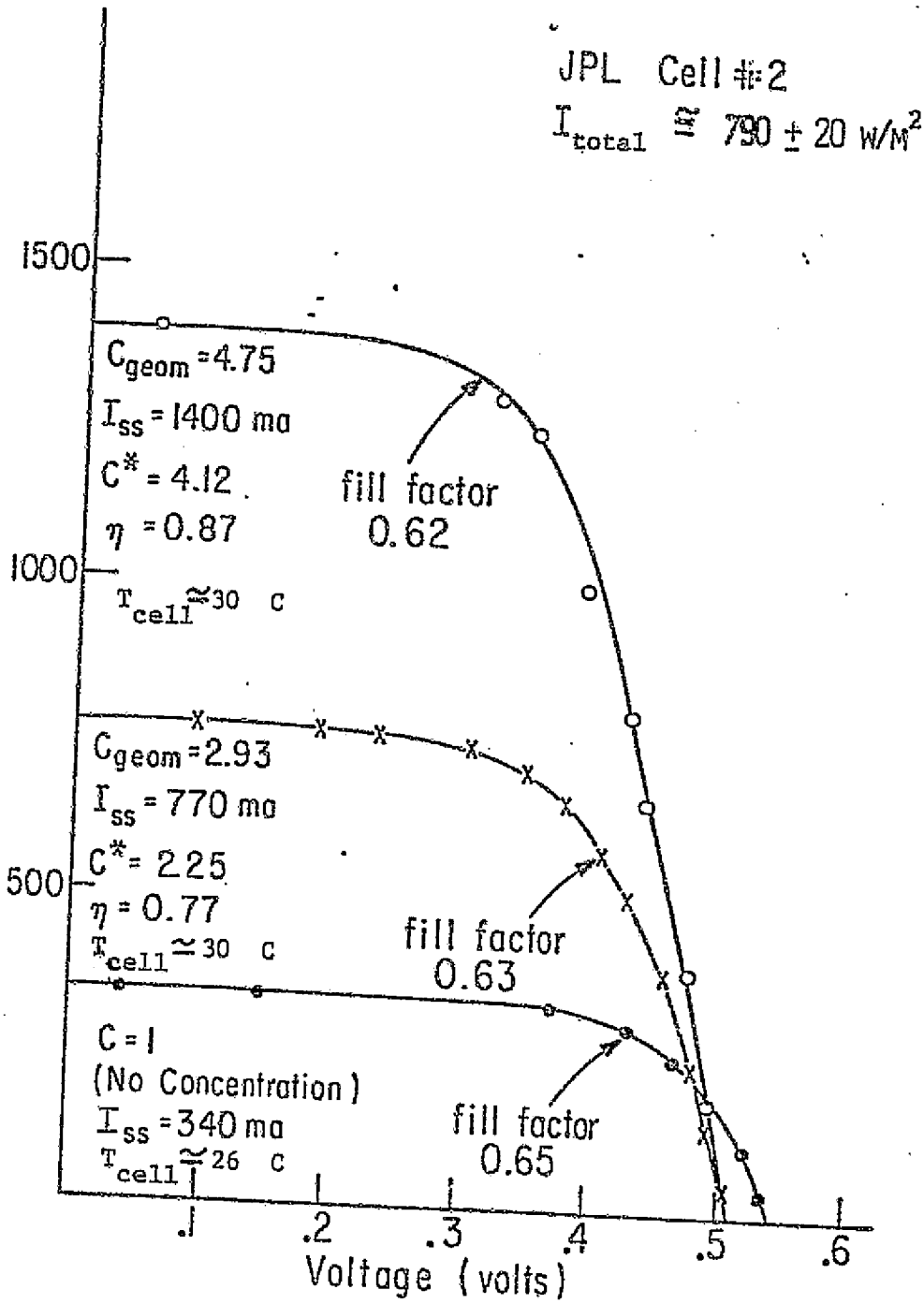

FIGURE 3 EFFECT OF CONCENTRATION ON I-V CURVE

short circuit current is shown in Figure 4. The slight rounding near $\pm 5^{\circ}$ is due to the finite angular width of the sun and some mirror errors in a molded plastic reflector. It should be emphasized that the performance illustrated in Figures 3 and 4 is characteristic of a single cell even with non-uniformities.

B. Selected Baseline Configuration

Following analysis of the small specimen concentrator behavior, the JPL staff elected to pursue a design option for a cometary mission utilizing one large concentrator for a wide multi-cell array rather than attempting to incorporate many small concentrators into the array itself. The width of the array blanket of the selected baseline design was 4 meters. The University of Chicago was instructed to design a CPC for an absorber blanket of this width having an accepting angle of $\pm 5^{\circ}$ and a geometric concentration ratio of 4.67 X. This concentration was selected in order to allow for expected reflection losses and those losses due to scattering from the non specular mirror surface proposed to reduce intensity non-uniformities. The profile curve for a CPC with the parameters is shown in Figure 5. This design has an acceptance angle ($\pm$ 5°) sufficient to provide mirror and pointing error tolerances for expected dynamic motions (i.e., "wet noodle") of a long ultra light weight blanket and reflector trough.

C. Variable Concentration Ratio

Following a suggestion by E. Costogue of JPL, the CPC design with this nominal concentration can be continuously varied down over a

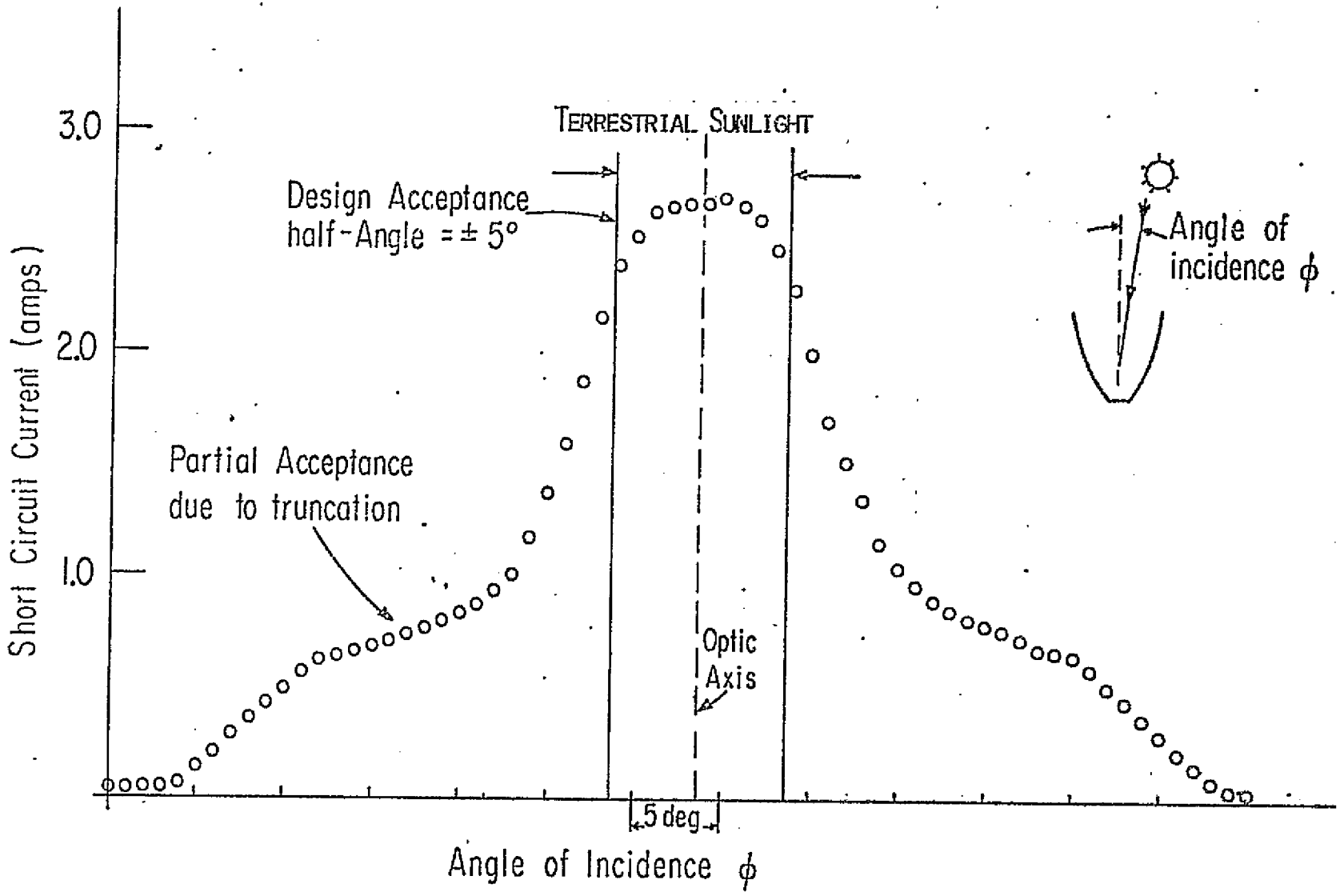

FIGURE 4 ANGULAR RESPONSE OF A 5X CPC

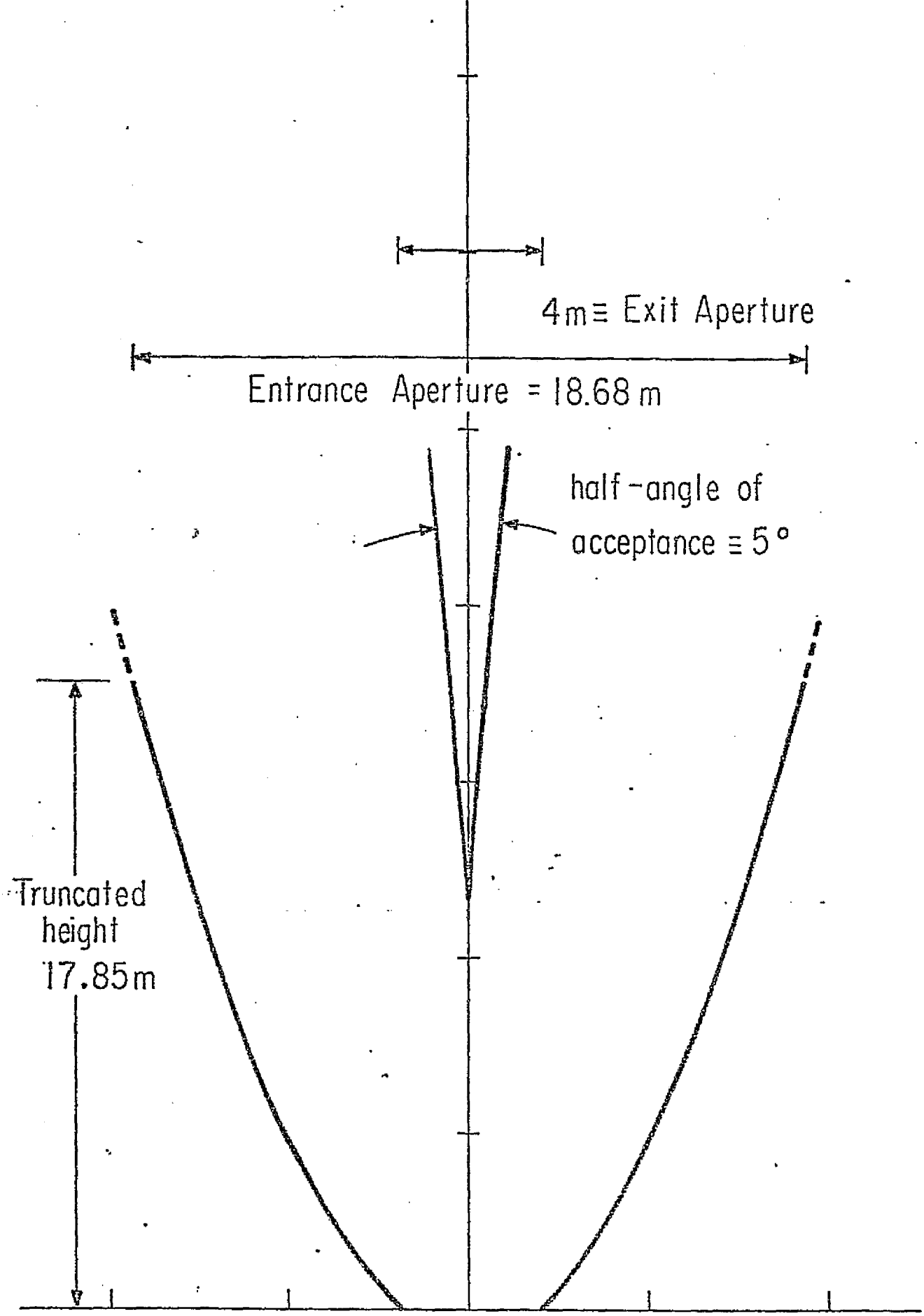

FIGURE 5 PROFILE OF 4.67 X CPC SPACE CONCENTRATOR

range of reduced concentration ratios extending to ~ 2 X simply by closing the aperture. This is done by pivoting reflector sides in, as if they were hinged about the lower mirror edge as shown in Figure 6. Such variable concentration is desired for deep space missions to control the average intensity on the cell blanket at increasing heliocentric distances beyond 1 astronomical unit. The CPC is particularly effective in accomplishing this requirement since at concentrations lower than nominal the optic axes of the parabolae tilt further out increasing the effective angular acceptance and insuring that every ray entering the new acceptance angle will reach the absorber blanket.

D. The Problem of Non-Uniformities

In general, optical concentrators designed to accept light over even a small range of incidence angles, will produce non-uniform intensity distributions on the absorber surface for most incident angles within the acceptance range. In the case of a CPC, the fundamental optical principles are such that if the acceptance half angle were filled uniformly with incident radiation, the intensity distribution on the absorber would be flat. But collimated radiation consisting of an effectively parallel beam incident at only one specific angle (such as from the sun at 1 a.u. with an angular spread of $\pm$ 1/4°) produces intensity peaks on the absorber from reflections from one or both mirrors. An example of the pattern produced if the mirrors are perfectly specular (smooth) is shown in Figure 7a. For the baseline CPC shown in Figure 5 this effect can be visualized as resulting from the fact that each parabolic side segment has a focus at the edge of the opposite side of the exit aperture for light incident presently at the acceptance angle. For

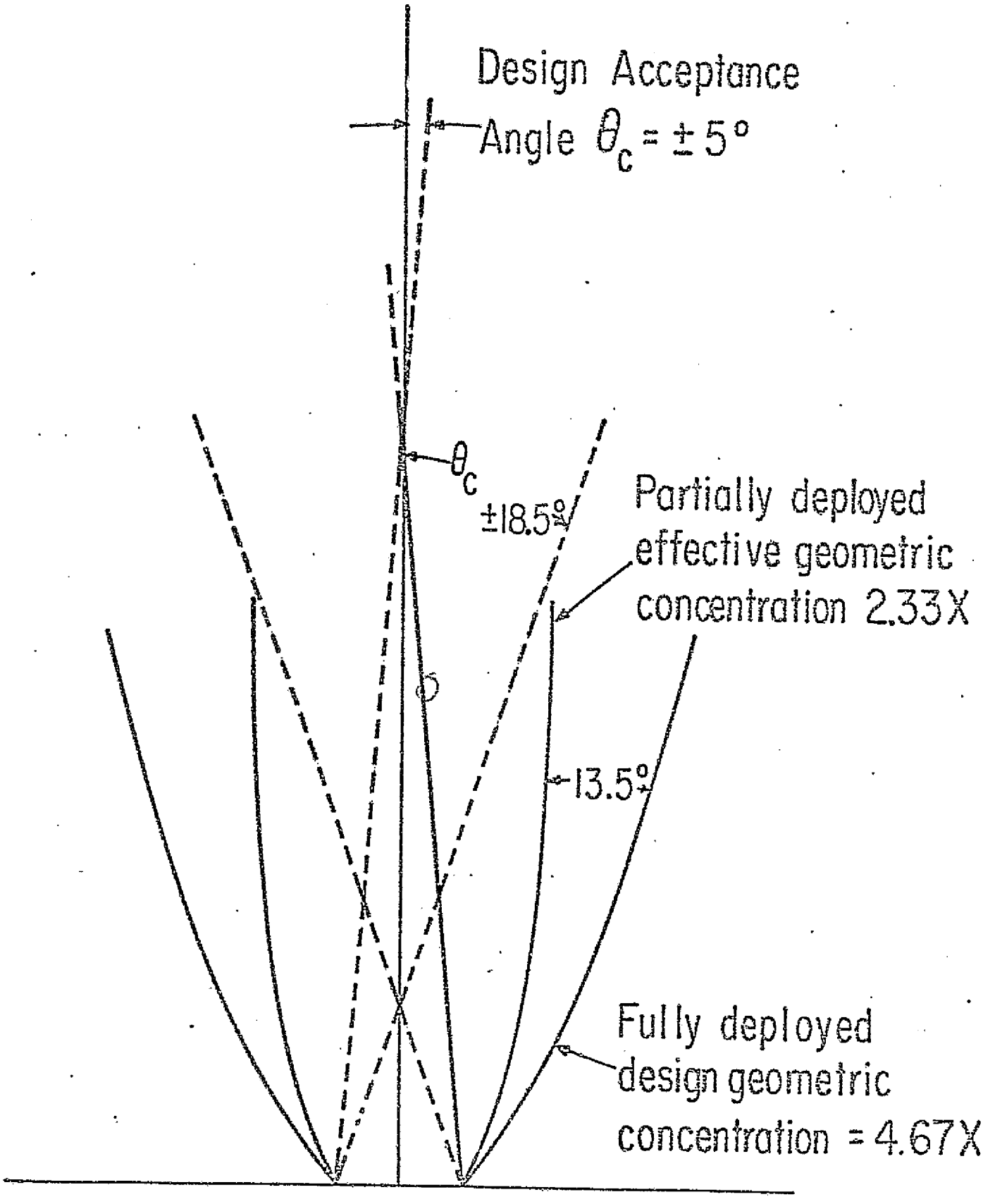

FIGURE 6 METHOD OF CPC CONCENTRATION REDUCTION

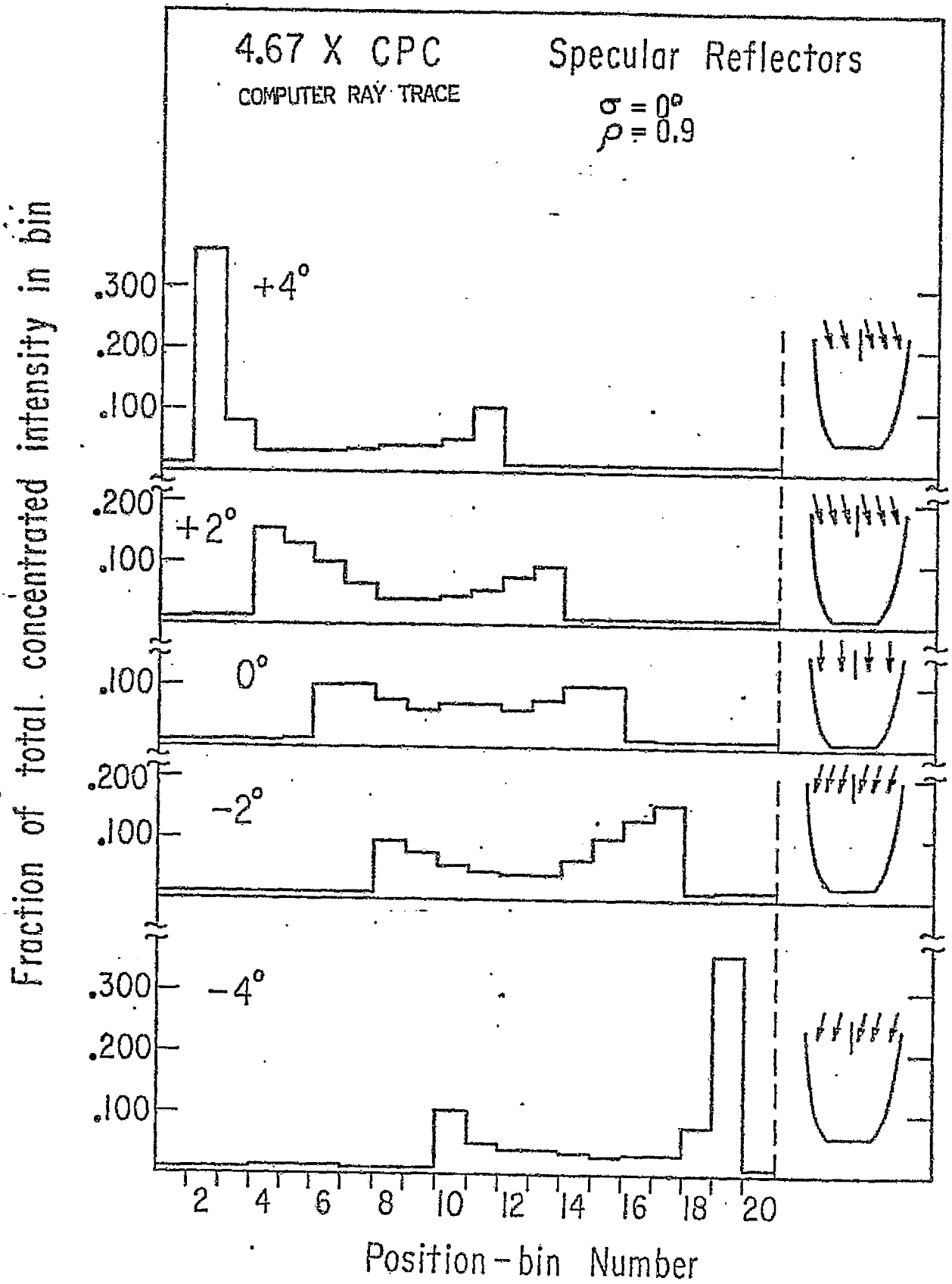

FIGURE 7A CALCULATED INTENSITY DISTRIBUTION: SPECULAR REFLECTOR

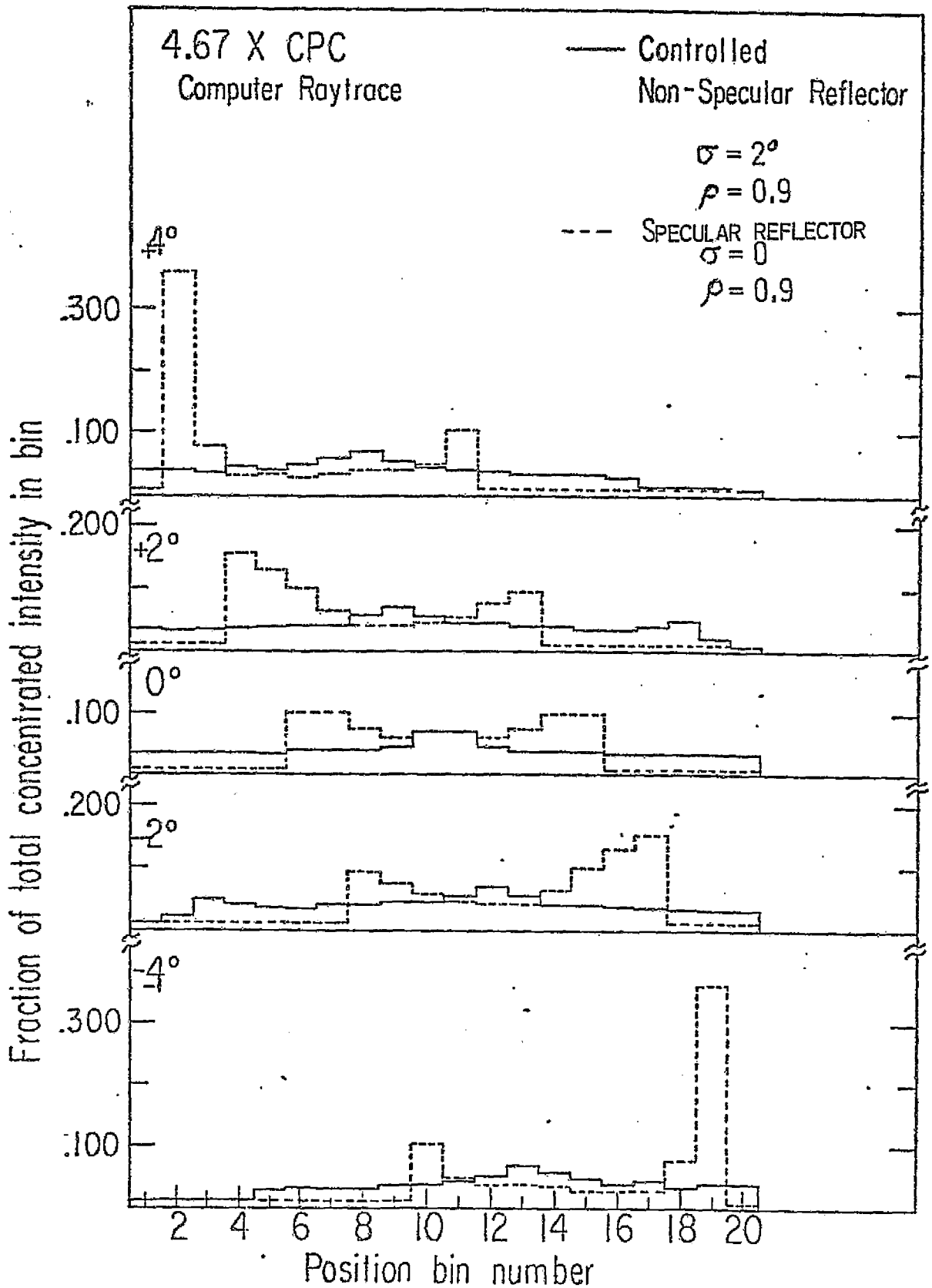

FIGURE 7B CALCULATED INTENSITY DISTRIBUTION: SPECULAR AND MODERATELY NON-SPECULAR SURFACE

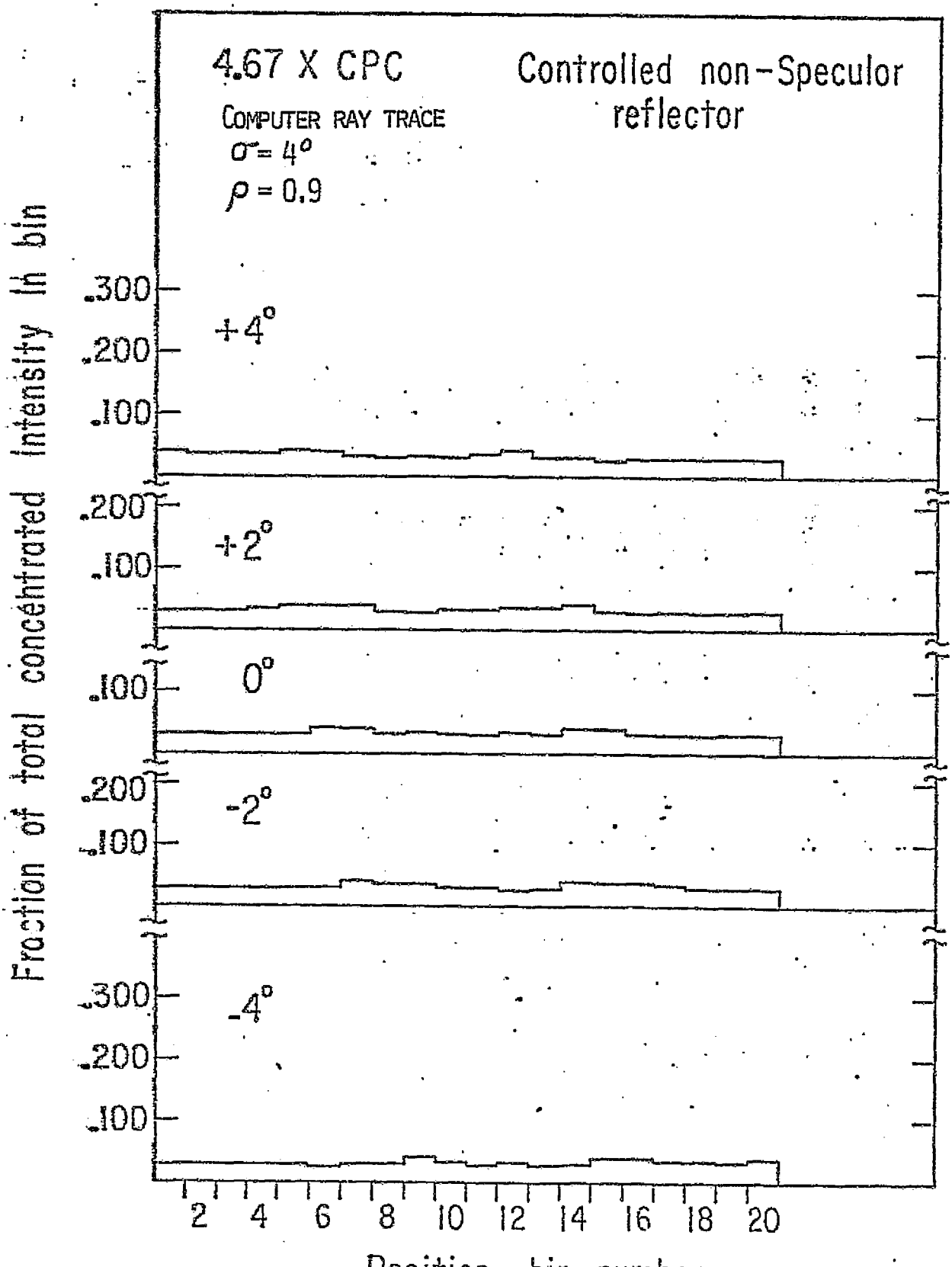

FIGURE 7C

CALCULATED INTENSITY DISTRIBUTION: RELATIVE NON-SPECULARITY TWICE THAT IN 7B

rays between the two extreme angles, these rays although now partially defocussed still tend to peak somewhere in the exit plane. Thus, for example, at $\theta = +4°$ or (just inside the acceptance angle) the majority of the rays are reflected on the right hand mirror resulting in a large peak near the left edge of the absorber surface. A small peak near the center results from the rays that strike the left mirror. As the angle of incidence is reduced, the large peak shrinks and the small peak grows and the distribution becomes symmetric at $\theta = 0$ with the left peak being produced by reflections off the right mirror and vice-versa.

The distributions in Figure 7a,b,c have been analytically calculated using a Monte Carlo ray trace technique which follows 5000 rays incident at random points on the aperture at the designated incidence angle and accumulates the number of rays hitting the absorber in each of 20 position bins across the exit plane. The resulting histograms are normalized so that the abcissa represents the relative fraction of the incident rays which end up in a given bin. To calculate the actual intensity then the fraction in a given bin should be multiplied by the concentration and the incident solar intensity and divided by the bin width. For example, if there is 1/2 solar constant incident at $\pm 2°$ on a concentrator with reflectors with reflectivity $\rho = 0.9$, the peak intensity would be $0.15 \times 4.67 \times 0.5/.05 = 7$ solar constants if no attempt was made to reduce the "peak to valley" ratio.

Note in particular, that the distributions in Figure 7a,b,c are in the transverse direction between the lower edges of the mirror concentrator and that at a fixed incidence angle, the variation is in this direction only. That is, at a fixed position between the edges, the intensity along the bottom of the trough in the longitudinal direction

(perpendicular to the page) is constant.

The problems associated with this non-uniform intensity distribution are mainly that for a multi-cell array, the performance of adjacent cells may not be well matched and the array is limited by the output of the poorly illuminated cells. The effect may be somewhat offset by a proper interconnect strategy, i.e., connecting cells across the width of the array in parallel so that their currents add, and along the length of the array in series. Further porblems can be caused by "hot spots" resulting in high cell temperatures and associated degraded performance.

E. A Solution to Reduce Intensity Variations

One method for reducing the size of relative intensity variations is to artificially "fill" the acceptance angle of the CPC concentrator by introducing a small amplitude angular scattering in the reflector surface about the nominal specular direction. This method of "controlled non-specularity" is illustrated in Figure 8 where the heavy line represents the profile curve of the theoretically perfect mirror. There will always be some small deviations from this "perfectly specular" surface but by intentionally introducing irregularities in the surface which have a root-mean squared angular deviation σ from the specular slope, where σ is a non-negligible fraction of design acceptance. (e.g. $0.1\ \theta_c \leq \sigma \leq 0.9\ \theta_c$), one can produce resulting distributions as if the incident light were spread out by $\sim \pm 2\sigma$ reducing "peaks" and filling "valleys" and thus being subtantially smoother than for specular mirrors. Of course

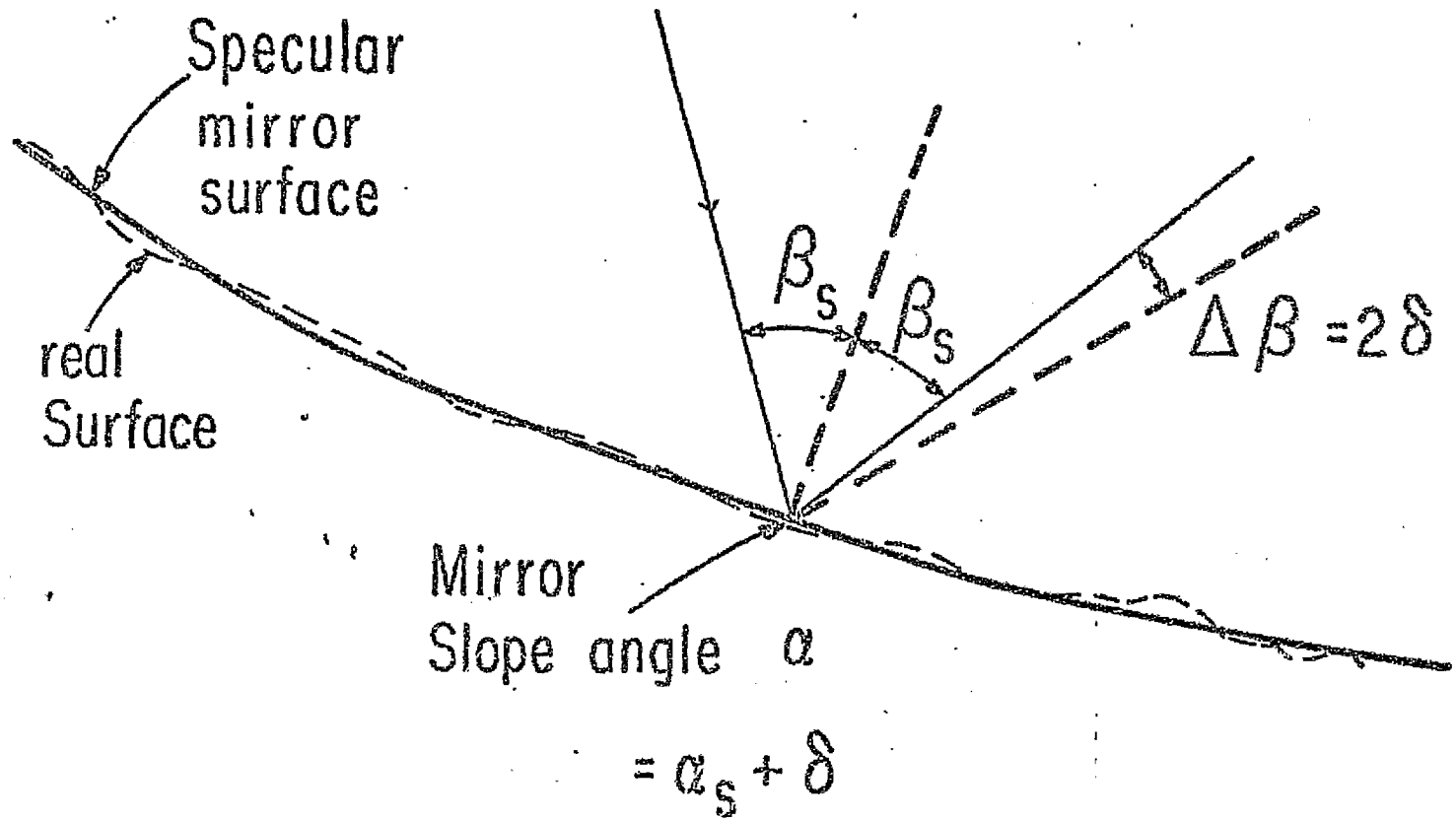

Gaussian Model

std. dev σ

$$P(\delta) = \frac{1}{\sqrt{2\pi}\sigma} e^{-\delta^2/2\sigma^2}$$

or

Sinusoidal $\delta = \sqrt{2}\,\sigma \sin(\phi) \qquad \phi \leq \phi \leq 2\pi$

FIGURE 8

METHOD OF CONTROLLED NON-SPECULARITY

some light rays will now be lost by being scattered back out of the concentrator,but if the amplitude of the average distribution can be controlled,the trade off between reduction of uniformities and some percentage loss in collection can be optimized. In principle, a value of σ equal to $\sim \theta_c/2$ should result in very effective smoothing without prohibitive scattering losses.

The qualitative effect of this solution has been analyzed extensively using further Monte-Carlo ray trace studies in which the slope of the reflector surface is modeled to have a given degree of non-specularity. Two different mathematical models were used to characterize the surface deviations; one a Gaussian probability distribution and one a sinusoidal surface model.

The effectiveness of the technique for the baseline $\theta_c = \pm 5°$ CPC configuration is illustrated in the computer generated distributions shown in Figures 7b and c, for root-mean-squared non-specularity parameters $\sigma = 2^o$ and 4^o respectively. The distribution for specular reflectors is shown dotted in Fig. 7b for comparison. Note that peak to valley ratios which ranged from 8:1 to 16:1 for specular reflectors are reduced to $\pm$ 30% for $\sigma = 2^o$ and $\pm$ 10% for $\sigma = 4$.

Of course, as noted above, there are some optical losses resulting from back-scatter of some rays within the nominal acceptance angle. This effect is illustrated in the angular acceptance (fraction of light reaching cell blanket as function of incidence angle) behavior calculated and shown in Figure 9. The integral under the curves for $\sigma = 2^o$ and 4^o is 17% and 27% less than under that for smooth reflectors respectively

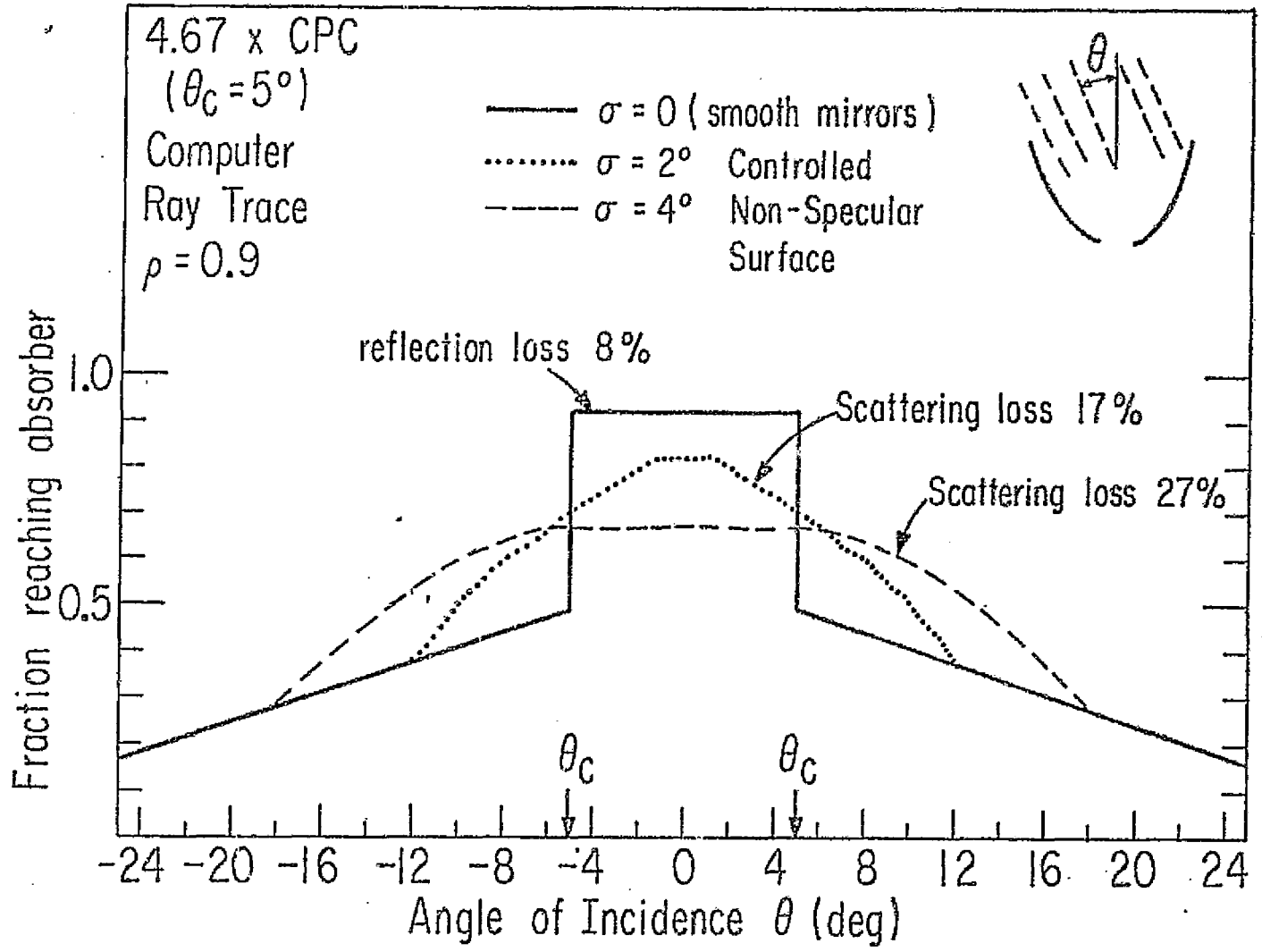

FIGURE 9 CALCULATED ANGULAR RESPONSE OF CPC WITH VARIOUS REFLECTOR SURFACES

and the acceptances are even broader. Note that a mirror reflectivity (ρ) of 0.9 has been included for all reflections in the ray trace program so even the smooth mirror case collects less than 100% (in this case 92%) of the incident light. (A fraction of about 1/C of the incident light reaches the absorber after no reflections so that the collection efficiency is greater than 0.9.)

These computer results verify that the proposed solution is conceptually sound and that the trade-offs between reductions in intensity variations and optical losses are quite acceptable. As will be discussed below, direct experimental measurements in terrestrial sunshine confirm the validity and accuracy of these predictions.

III. Experimental Measurements

A. Test at General Electric Space Division, Valley Forge Pennsylvania, February 2-3, 1978

As part of the contracted effort our staff participated in the scheduled tests of a CPC concentrator model conducted at General Electric in early February. The tests were conducted with a CPC trough using 7 mil thick specular Al mylar foil reflectors held by ribs shaped to the 1/50 scale model 4.67 X template fabricated by University of Chicago in Phase I. A schematic diagram of the test model is shown in Fig. 10a. (The second reflector is not shown for clarity.) The ribs were hinged along the lower edge in order to vary the effective geometric concentration. No attempt was made to reduce intensity variation on the absorber plane although it should be noted that the G.E. solar simulator beam had an angular divergence of $\Delta\theta \cong \pm 2°$ and so, does not truly represent the extreme collimation of sunlight.

The absorber itself was divided into two halves: a) an 80 cell module (4 cells x 20 cells each 2 cm x 2 cm) to investigate the behavior of a multi-cell array; and b) a single cell on a moveable prove to scan the intensity distributions in both the longitudinal and transverse directions for the worst case conditions.

The results of the tests are summarized in Figures 10, 11, and 12.

Figure 10 illustrates the transverse intensity distributions as measured by the single cell probe (short-circuit current) at 8 longitudinal positions (A-H) along the length of the trough both for full nominal geometrical concentration ($C_g = 4.67$) (left panel) and with the "clamshell" aperture closed down to $C_g \cong 1.75$ (right panel). The distributions predicted by ray trace techniques for smooth reflec-

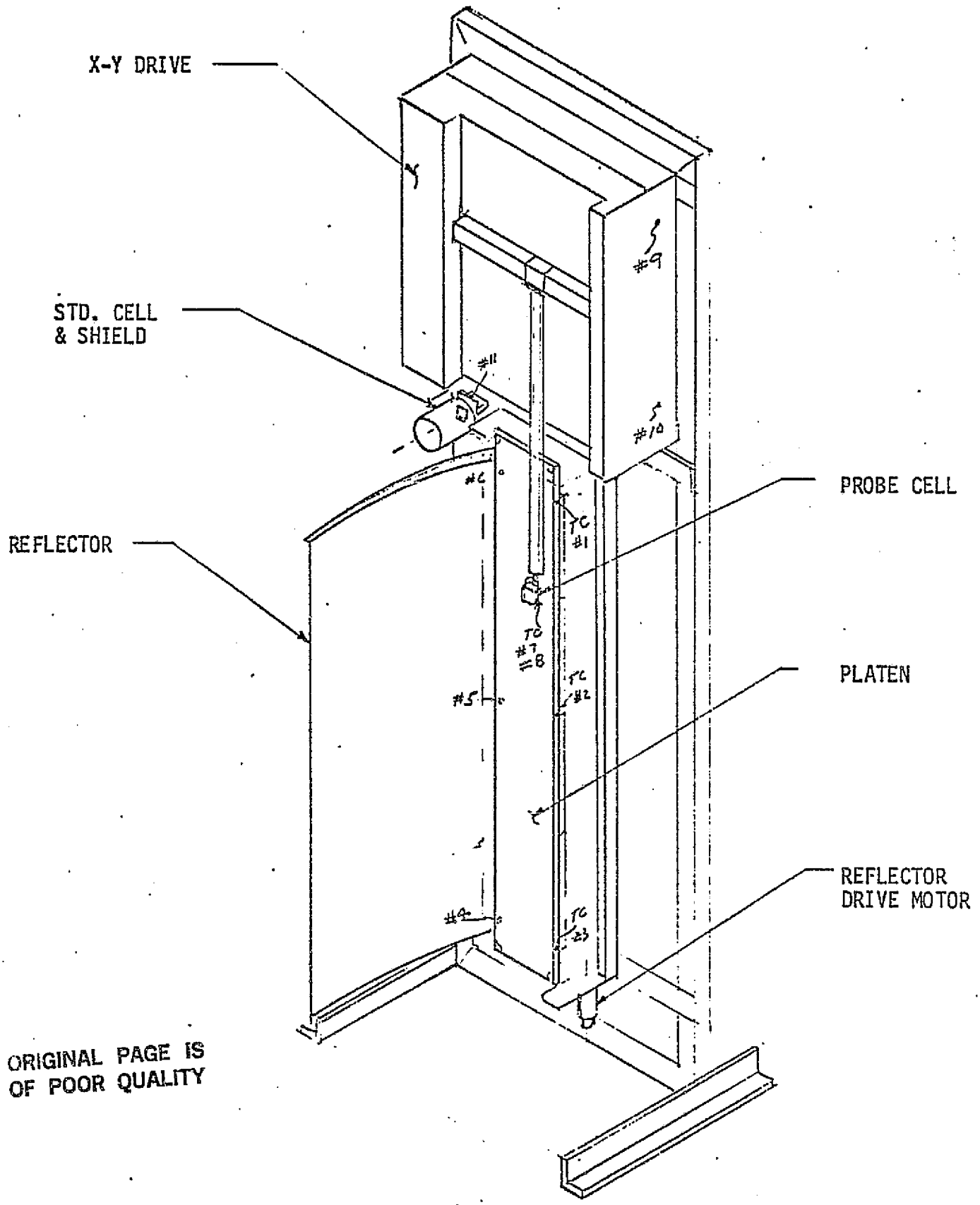

ORIGINAL PAGE IS
OF POOR QUALITY

FIGURE 10A G.E. TEST FIXTURE ASSEMBLY

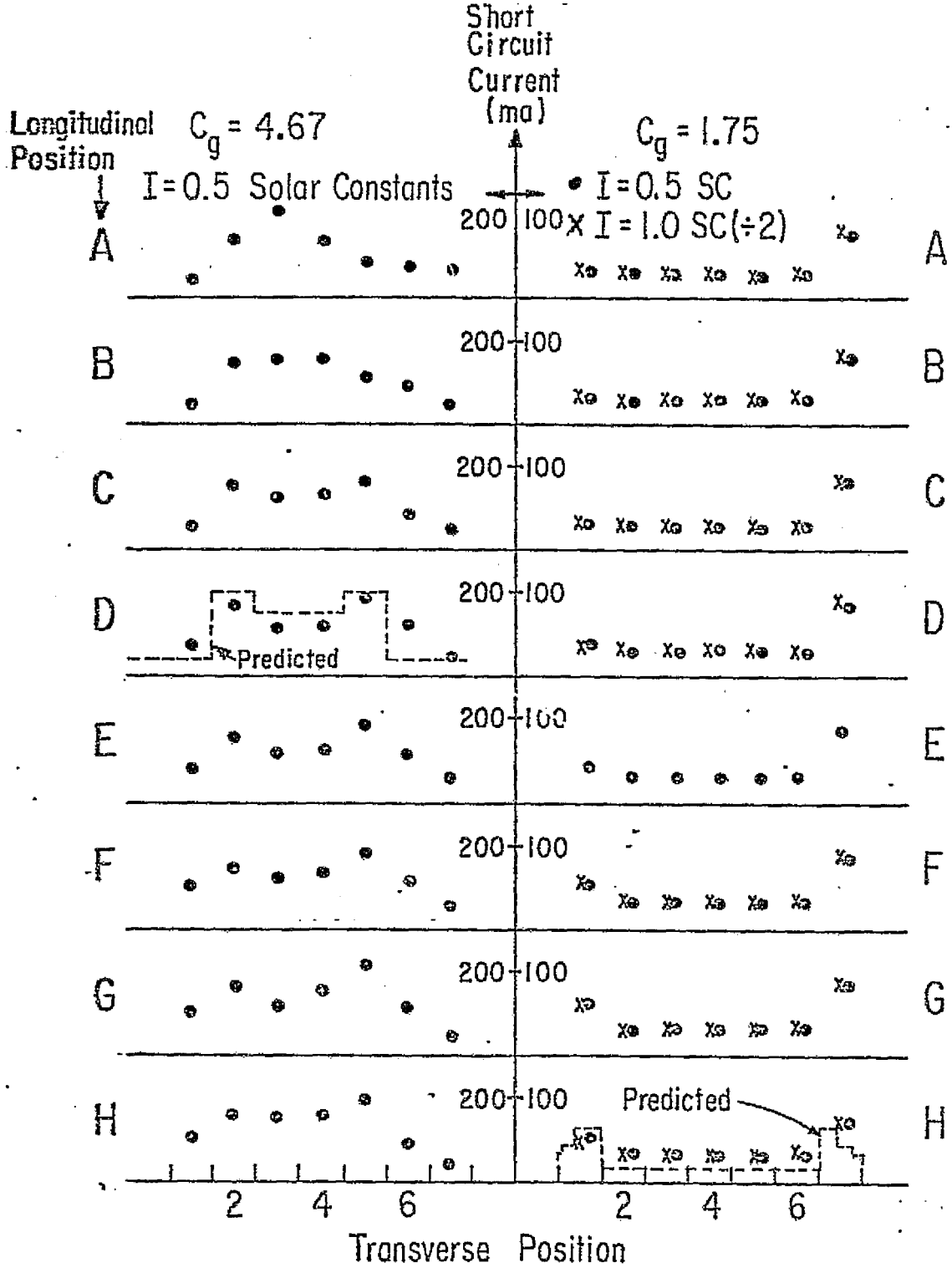

FIGURE 10B MODEL TESTS AT G.E.: INTENSITY DISTRIBUTION ACROSS CELL BLANKET

tors are shown by the dotted lines superimposed on two of the measured distributions. The most important features are summarized below:

1) the general pattern is as expected with the characteristic two peak distribution being quite evident.

2) There is clearly some twisting or skewing of the mirror surfaces from one end to the other about the longitudinal axis as is evident from the distorted distribution in panels A and B, giving rise to longitudinal variations as well.

3) The distribution is quite flat for $C_{geom} = 1.75$ except at the outer edges.

4) The slight asymmetry of all the distributions indicates that the concentrator was probably misaligned slightly.

5) The shape of the distribution is independent of illumination (as, of course, it must be for the optics), indicating that the cell current responds linearly to intensity over the observed range.

6) The maximum intensity variations under the simulated conditions are typically between 3:1 and 4:1.

Figure 11 illustrates the response of the 80 cell array connected in a parallel-series (transverse-longitudinal) configuration under concentration. The lower curve is for no concentration under 1.0 solar constant and the upper is for $C_{geom} = 4.67$ under 0.5 sun illumination. For plotting, the lower curve has been normalized by dividing the measured current by 2. The measured optical gain (from short circuit current gain) is in excellent agreement with that predicted from

$$C_{eff} = C_{geom} \cdot (\rho)^{<n>} \qquad (3)$$

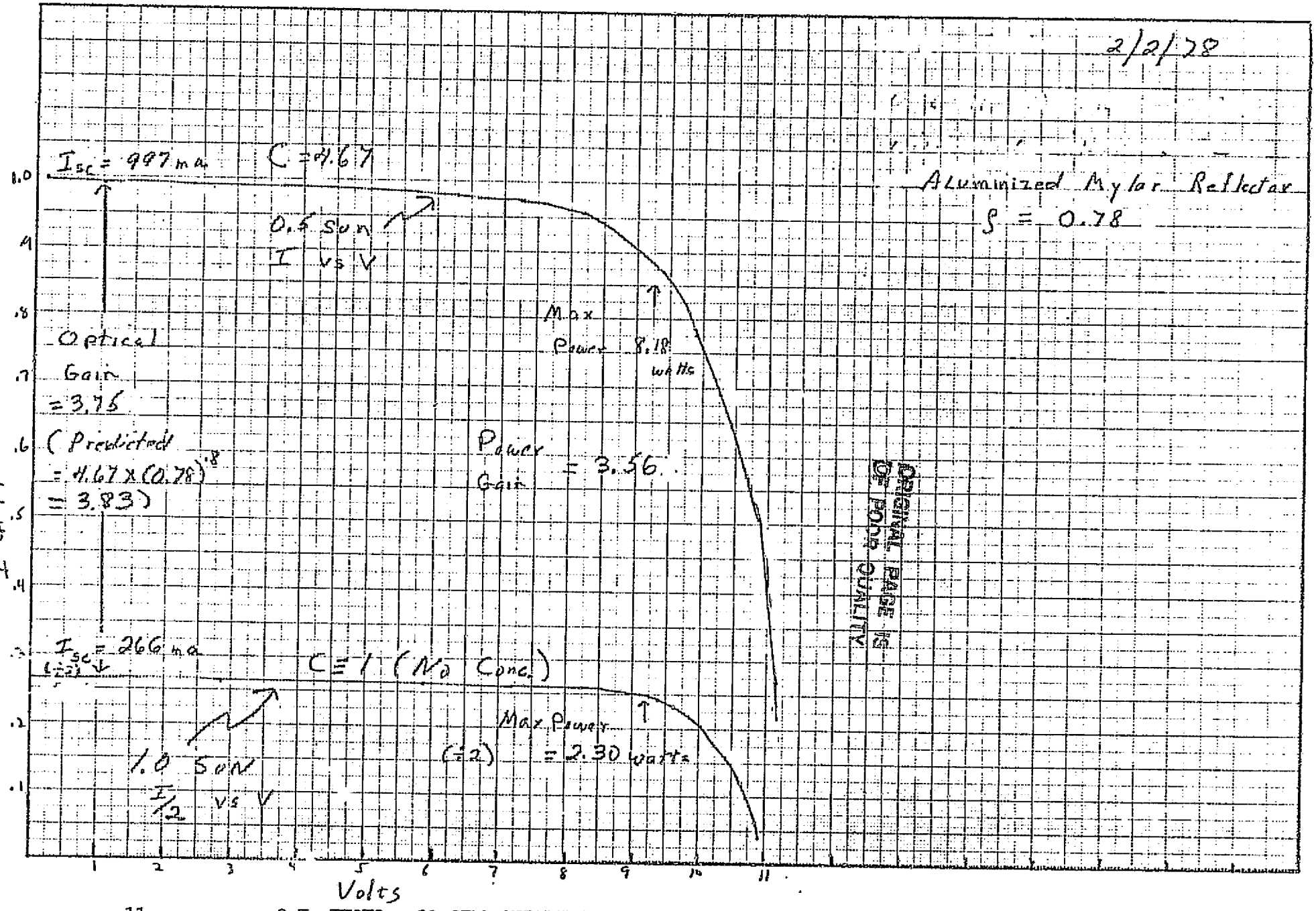

FIGURE 11 G.E. TESTS: 30 CELL MODULE RESPONSE WITH AND WITHOUT CPC

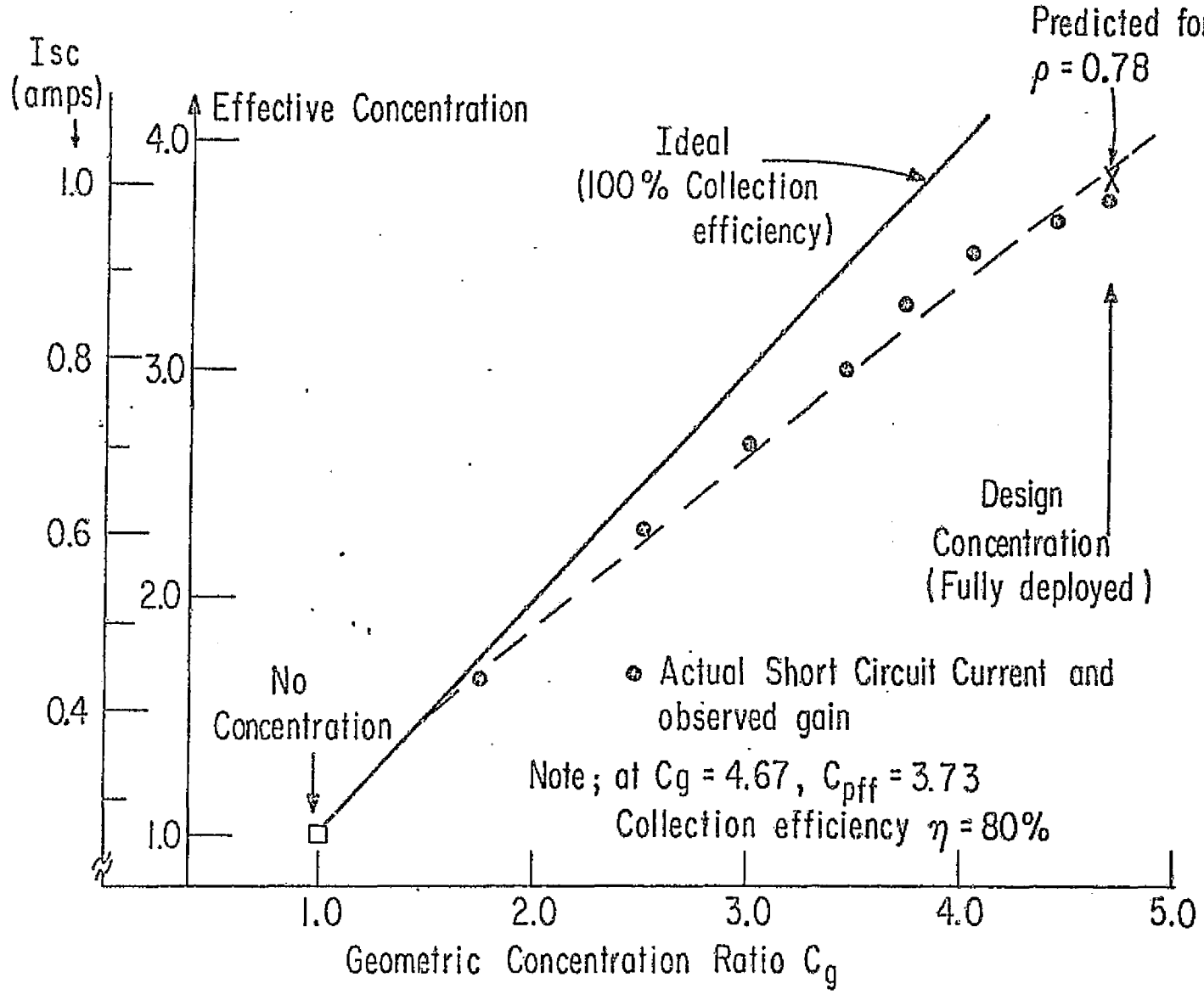

FIGURE 12 MODEL TESTS AT G.E.: CELL RESPONSE UNDER VARIABLE CONCENTRATION

where ρ is the reflectivity (here = 0.78) and $\langle n \rangle$ is the average number of reflection ($= 1 - 1/C$). The power gain is slightly less due to a small rounding of the I-V curve knee under concentration. It should be emphasized that this behavior is observed in the presence of substantial (3:1 to 4:1) non-uniformities on the cell blanket.

The measured effectiveness of the implementation of variable concentration as suggested by E. Costogue of JPL is shown in Figure 12; where the effective gain in short circuit current is plotted against the ratio of the aperture area to cell blanket width as the aperture is varied from a low of 1.75 X to the nominal of 4.67 X. The solid line shows the expected optical gain for perfect ($\rho = 1.0$) reflectors. The observed gains are in precise agreement with the calculated gains based on the reflectivity of $\rho = 0.78$ measured for a sample of the actual reflectors. The low value of ρ is due to some contamination (a thin oil film) which was generated in the simulation chamber.

B. Tests at the University of Chicago, February - June 1978

The above tests at G.E., while measuring characteristics of variations and demonstrating the performance of a real cell array under variable concentration are incomplete in that: a) the incident light was not strongly collimated; and b) no attempt was made to investigate the effectiveness of non-specular reflectors in reducing non-uniformities.

A model CPC from the same template was built at the University of Chicago in order to complement the G.E. tests by measuring intensity distributions in terrestrial sunshine (effectively $\pm$ 1/4° collimation) and with interchangeability among selected non-specular reflector foil surfaces. The model utilized a metal form, shaped to the proper tem-

plate, whose surface was perforated with many small holes. The supporting structure was enclosed and attached to a small shop vacuum which then held the desired sample reflector materials against the shaped surface.

The reflecting foils tested were all of Mylar of various thickness. A set of reference measurements was made with smooth foil directly off the roller for each thickness. Other samples were formed whose surfaces were "corrugated" by passing them over a roller and against a ridged cylinder which produced permanent indentation in the foil. Several-thickness foils and several values for the spacing of the corrugations were tried.

The characteristic scattering angle for each of the surfaces was measured by measuring the dispersion in the location of a normally incident laser beam reflected from its surface at a fixed distance. Values of σ in the range 2^{o} - 3^{o} generally resulted from the corrugation technique.

The total hermispherical reflectivity of the foil samples was also measured using a Beckman integrating sphere spectral reflectometer at Argonne yielding values in the range $\rho = 0.87 - 0.90$.

Tests of a wide variety of surfaces were conducted throughout the period. In general a dramatic reduction in the degree of intensity variation was observed when corrugated reflectors were used. These reductions were found to be in very good agreement with the calculated predictions based on ray trace results discussed in Section II above and confirm the validity of the computer method for extensions to other studies.

Some selected examples of these results are shown in Figures 13-15. Figure 13 shows the measured intensity distribution (short circuit current) with specular reflectors. The cell probe used was 2.5 mm wide within an 8 cm cut aperture or 1/32 of the aperture width. The histograms are the predicted distributions for "worst case" specular reflectors and are as large as 16:1. Contrast this with the distributions shown in Figure 14 which is the measured intensity (short circuit current) when corrugated 3 mil mylar with $\sigma \cong 2.5°$, $\rho = 0.87$ is used for the reflector. The dashed histogram is the corresponding ray trace prediction. Note again the excellent agreement between prediction and measurement. Here the intensity variations are no greater than ~ $\pm$ 20%. Figure 15 is the same as Figure 14 except that 0.5 mil mylar with a slightly smaller σ has been used which results in a slightly less flat interaction distribution.

An example of measured optical losses is plotted in the acceptance angle diagram in Figure 16. Here, as before, the corrugated mylar foil shows a good agreement with ray trace predictions and corresponds to a relative loss due to scattering of 18% as the price that must be paid to reduce the intensity peaks.

Finally, we note that these distributions should allow relatively even temperature distributions across the cell blanket as shown in Figure 17. Here, the equilibrium temperatures for an average intensity on the cell blanket of 1 solar constant = 135.3 mw/cm^2 calculated from a formula supplied by Don Rockey at JPL are plotted for the normalized measured relative intensity distribution on the blanket for smooth (open circles) and corrugated (crosses) reflectors. In the latter case temperatures in the range 20°c - 60°c are to be expected.

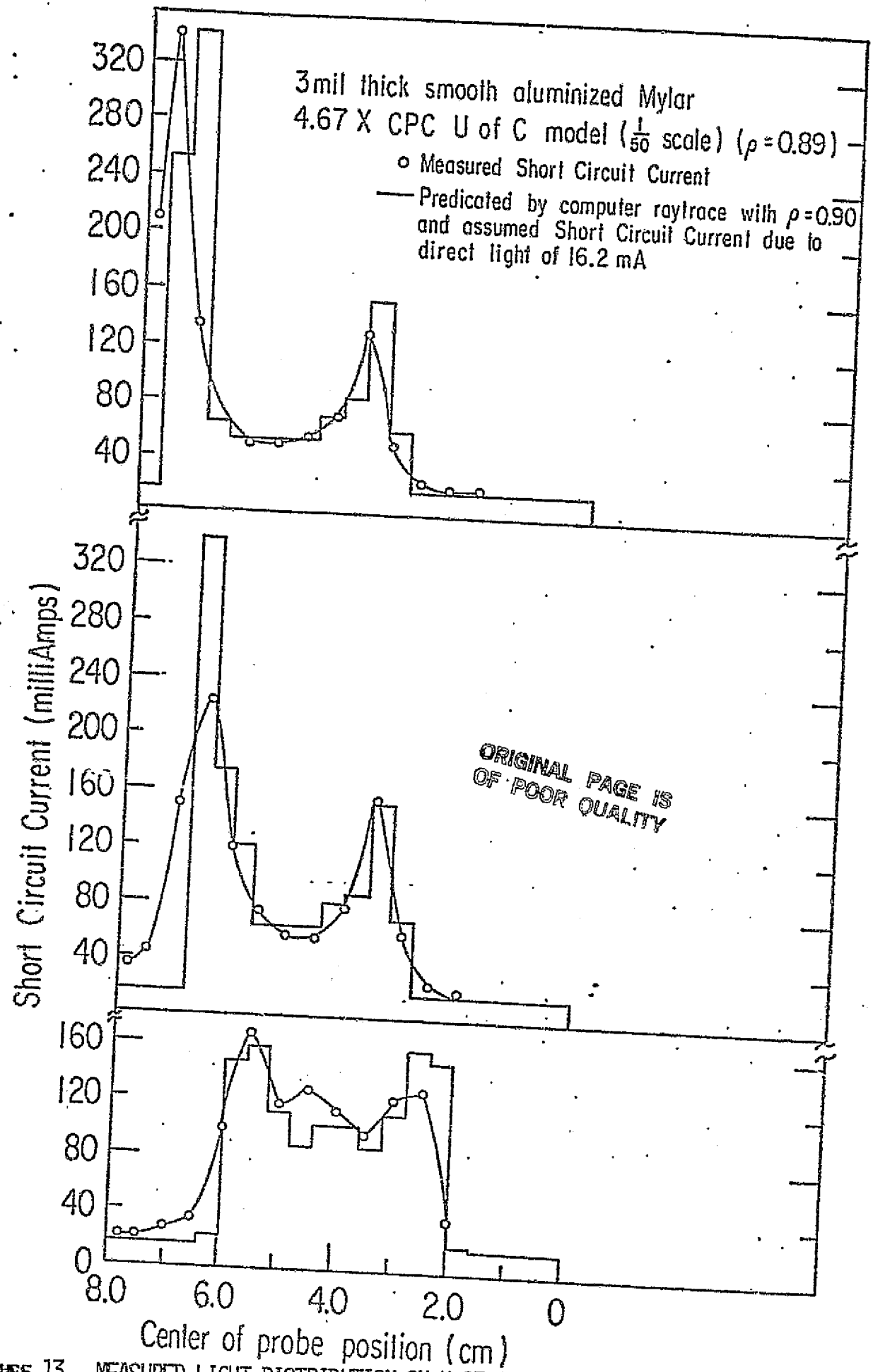

FIGURE 13 MEASURED LIGHT DISTRIBUTION ON U OF C MODEL: SMOOTH REFLECTORS

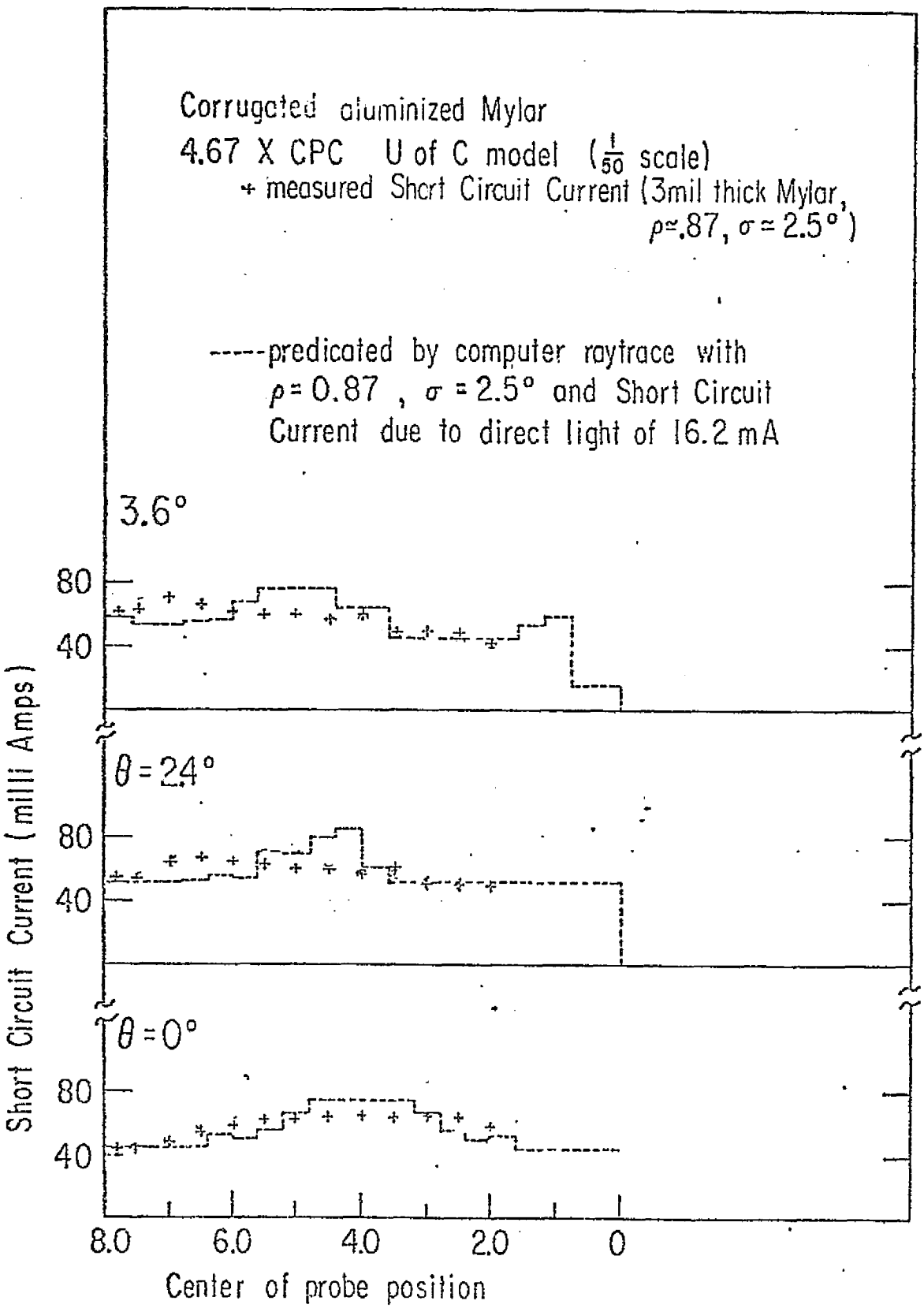

FIGURE 14 MEASURED LIGHT DISTRIBUTION ON U OF C MODEL: CORRUGATED REFLECTORS

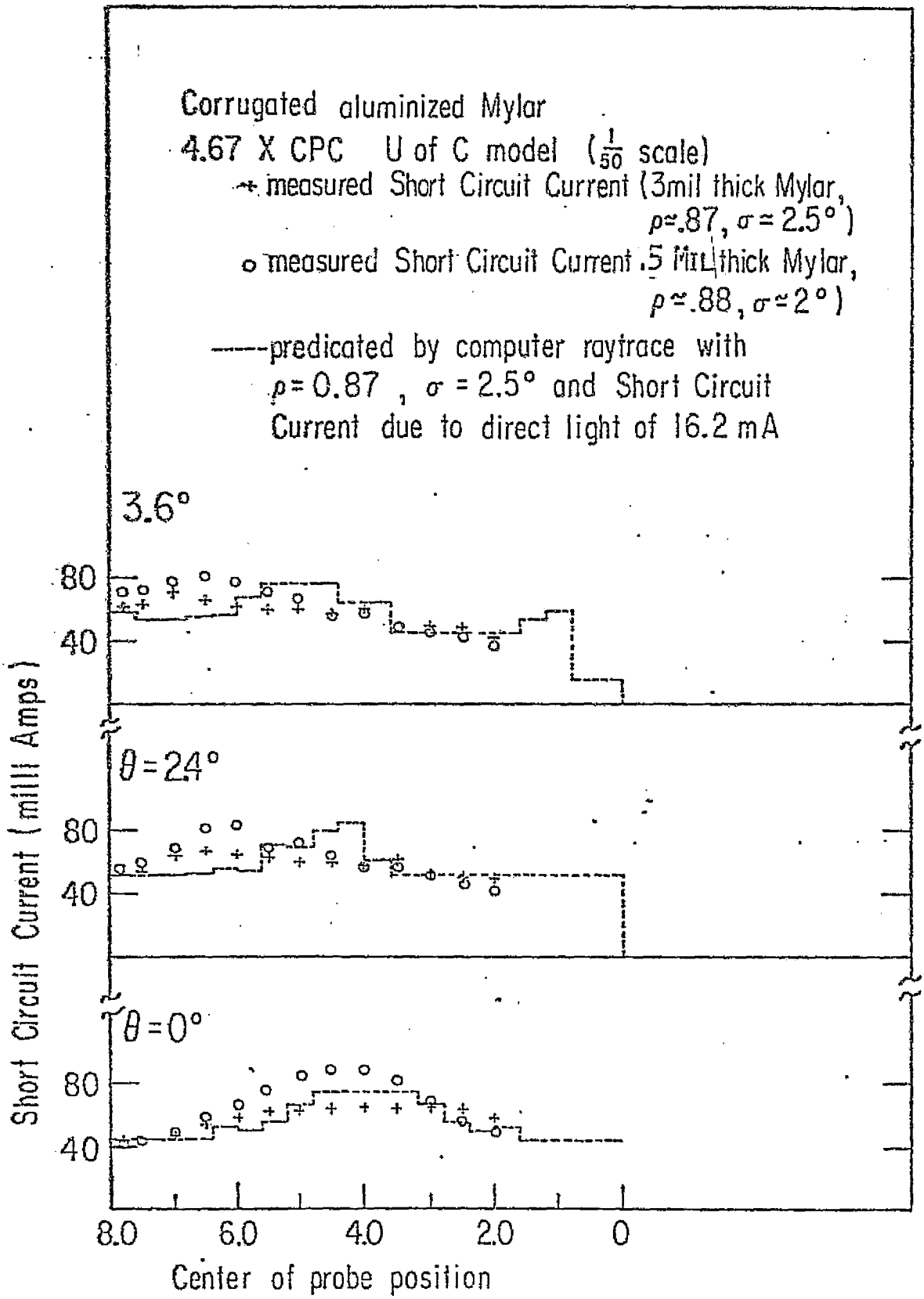

FIGURE 15 MEASURED LIGHT DISTRIBUTION ON U OF C MODEL: TWO TYPES OF CORRUGATED REFLECTORS

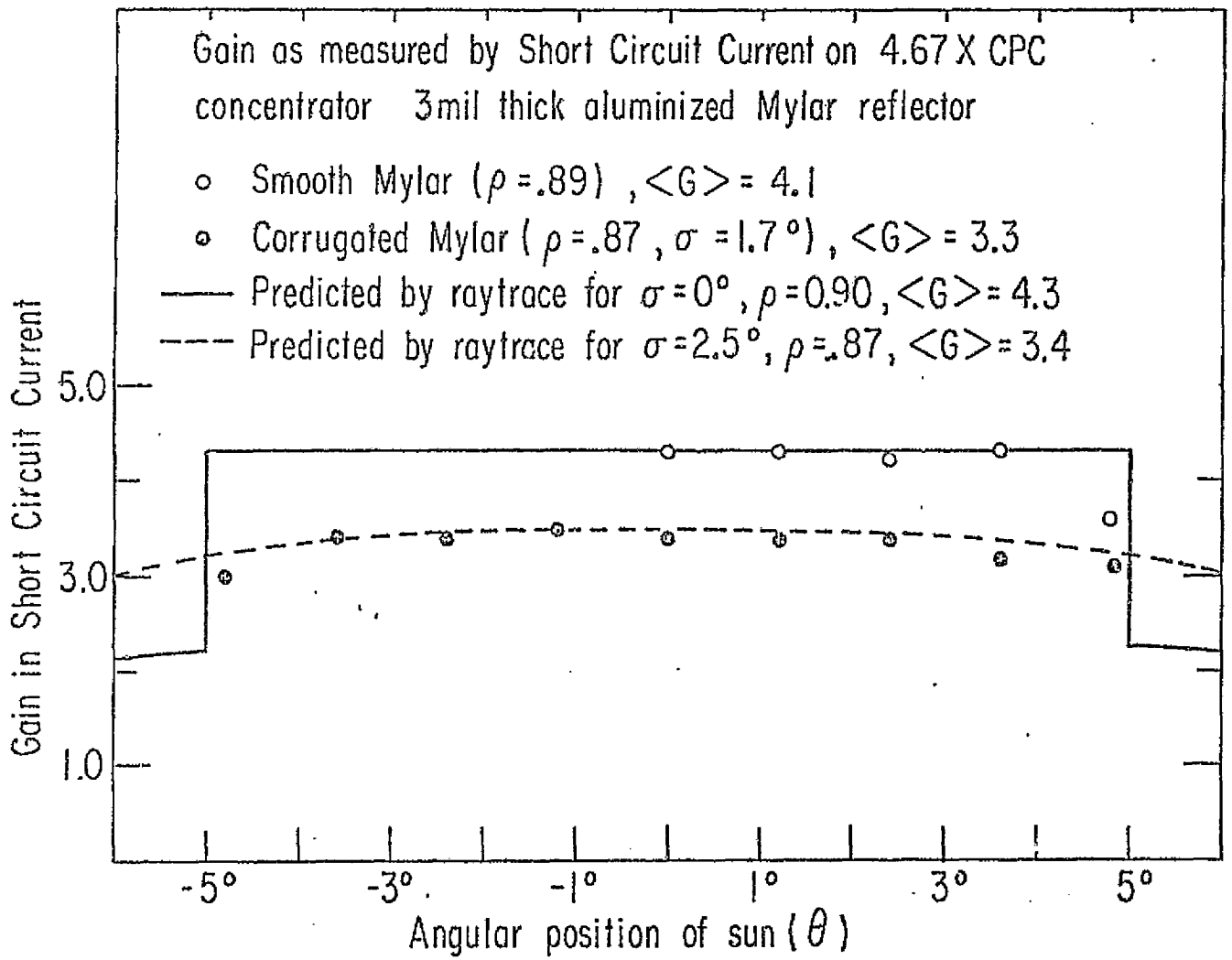

FIGURE 16 MEASURED ANGULAR RESPONSE OF U OF C MODEL

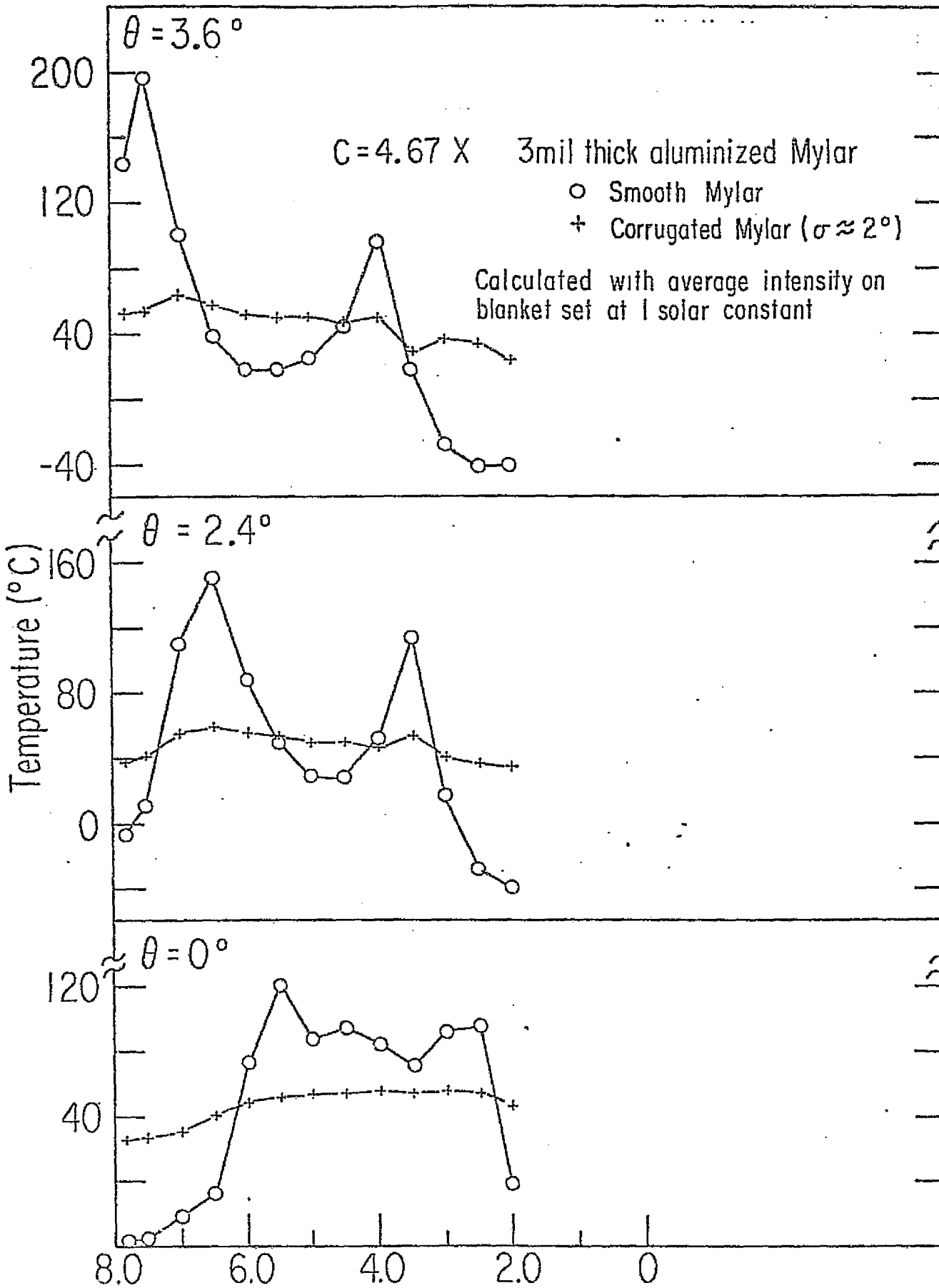

FIGURE 17

FIGURE 17 CALCULATED TEMPERATURE DISTRIBUTION (ON BLANKET OF SOLAR CELLS) BASED ON MEASURED INTENSITY DISTRIBUTION

The above results demonstrate unambiguously that 1) the introduction of small angle scattering is a practical effective method for reducing or eliminating non-uniformities as a potential problem for concentrator-cell arrays in space. 2) Analytical studies based on computer ray tracing are very reliable for predicting expected concentrator behavior, e.g., performance, intensity distributions, acceptance, etc.

IV. Extended Analytical Studies of Baseline Configuration

A set of ray trace analyses of the baseline configuration under various perturbations was performed to obtain a more complete understanding of its optical properties, behaviors and tolerances. In particular, the following four studies were carried out:

1) Calculation of the intensity distributions, with both specular ($\sigma = 0°$) and non-specular ($\sigma = 2°$) reflectors, on an extremely fine grid (100 bins) equivalent to a resolution of approximately two 2 cm wide cells on the scale of the baseline 4 m wide blanket. The distribution for $\theta = 0°$ is shown in Figure 18. The dramatically narrow peaks are effectively eliminated by the non specular reflection.

2) Calculation of the intensity distribution along the length as well as the width of the baseline CPC troughs under simulated distortion represented by a twist of one end of the concentrator array by a given angle while the other end is held fixed, pointed accurately at the sun (0° incidence). The angle of distortion was assumed to vary linearly with distance along the trough. The intensity distributions are presented in Table 1a-g in the form of a 10 x 10 matrix. Vertical columns in this table represent transverse slices across the intensity distribution taken at equally spaced intervals along the trough. The rows are samples from the distribution along the bottom of the trough at a fixed distance between the concentrator edges. The normalization is in arbitrary units. For reference, the first three data sets (a-c) are for the worst case specular mirror case. Values of twist angle (at the right hand edge of the distribution) of 0°, 2°, and 4° are shown. Note that as the array is twisted, the two intense parallel strips along the middle of the intensity distribution gradually shift

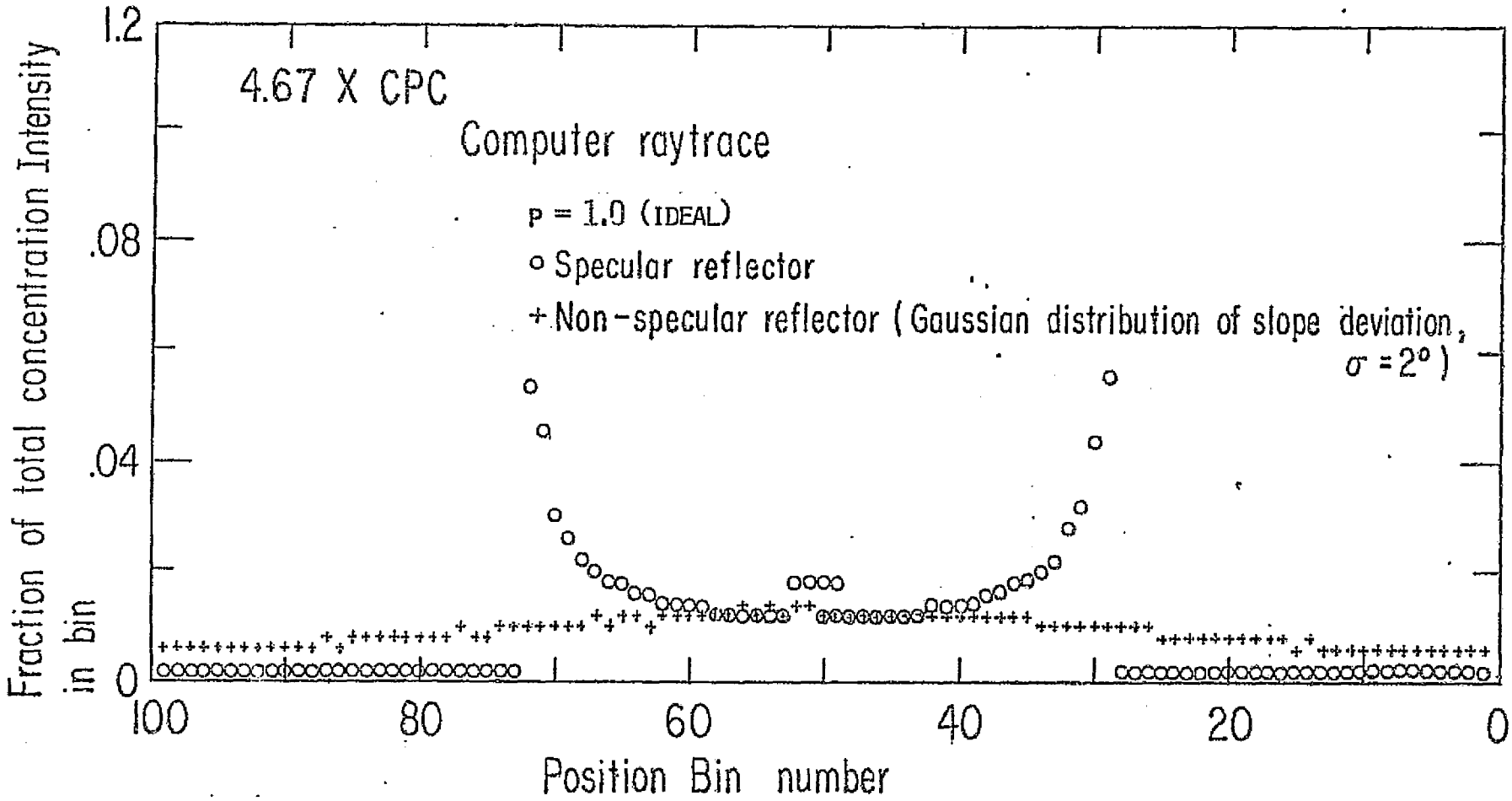

CALCULATED INTENSITY DISTRIBUTION,
SPECULAR AND NON-SPECULAR REFLECTORS (FINE BINNING)

FIGURE 18

TABLE 1A RELATIVE INTENSITY vs POSITION MATRIX

- SPECULAR REFLECTORS

- NO INDUCED DISTORTION (TWIST = 0^{0})

2	2	2	2	2	2	2	2	2	2	2
2	2	2	2	2	2	2	2	2	2	2
11	11	11	11	11	11	11	11	11	11	11
18	18	18	18	18	18	18	18	18	18	18
13	13	13	13	13	13	13	13	13	13	13
13	13	13	13	13	13	13	13	13	13	13
18	18	18	18	18	18	18	18	18	18	18
11	11	11	11	11	11	11	11	11	11	11
2	2	2	2	2	2	2	2	2	2	2
2	2	2	2	2	2	2	2	2	2	2

TRANSVERSE DIRECTION

LONGITUDINAL DIRECTION

TABLE 1B RELATIVE INTENSITY vs POSITION MATRIX

- SPECULAR REFLECTORS

- INDUCED DISTORTION (TWIST = 2^0)

TRANSVERSE DIRECTION	2	3	2	3	2	2	3	2	2	2	2
	2	2	2	3	2	3	2	2	2	11	16
	11	14	17	18	22	22	26	27	30	25	23
	18	17	16	15	15	15	16	15	14	12	11
	13	14	14	13	13	11	9	10	9	9	10
	13	11	11	11	12	12	11	13	12	13	13
	18	20	23	11	10	19	17	16	15	13	11
	11	7	2	2	2	2	2	2	2	2	2
	2	2	2	3	3	2	2	2	2	2	3
	2	2	2	2	2	2	2	2	2	2	2

LONGITUDINAL DIRECTION

TABLE 1c RELATIVE INTENSITY vs POSTION MATRIX

- SPECULAR REFLECTOR

- INDUCED DISTORTION (TWIST = 4^0)

TRANSVERSE DIRECTION	2	2	2	3	2	2	2	2	2	18	37
	2	2	2	2	2	16	24	33	40	27	11
	11	17	22	26	30	23	20	14	8	7	6
	18	16	15	16	14	11	8	7	7	7	8
	13	14	13	9	9	10	10	9	9	10	9
	13	11	12	11	12	13	16	17	16	14	11
	18	23	20	17	15	11	6	2	2	2	2
	11	2	2	2	2	2	2	2	2	2	3
	2	2	3	2	2	3	2	2	2	2	2
	2	2	2	2	2	2	2	2	2	2	1

LONGITUDINAL DIRECTION

TABLE 1D RELATIVE INTENSITY vs POSITION MATRIX

- NON-SPECULAR REFLECTOR ($\sigma = 2^0$)
- NO INDUCED DISTORTION (TWIST 0^0).

TRANSVERSE DIRECTION	7	7	7	7	7	7	7	7	7	7	7
	6	6	6	6	6	6	6	6	6	6	6
	7	7	7	7	7	7	7	7	7	7	7
	8	8	8	8	8	8	8	8	8	8	8
	11	11	11	11	11	11	11	11	11	11	11
	12	12	12	12	12	12	12	12	12	12	12
	8	8	8	8	8	8	8	8	8	8	8
	7	7	7	7	7	7	7	7	7	7	7
	7	7	7	7	7	7	7	7	7	7	7
	7	7	7	7	7	7	7	7	7	7	7

LONGITUDINAL DIRECTION

TABLE 1E RELATIVE INTENSITY vs POSITION MATRIX

- NON SPECULAR REFLECTOR ($\sigma = 4^0$)
- NO INDUCED DISTORTION (TWIST = 0^0)

6	6	6	6	6	6	6	6	6	6	6
6	6	6	6	6	6	6	6	6	6	6
8	8	8	8	8	8	8	8	8	8	8
7	7	7	7	7	7	7	7	7	7	7
6	6	6	6	6	6	6	6	6	6	6
6	6	6	6	6	6	6	6	6	6	6
7	7	7	7	7	7	7	7	7	7	7
7	7	7	7	7	7	7	7	7	7	7
6	6	6	6	6	6	6	6	6	6	6
6	6	6	6	6	6	6	6	6	6	6

TRANSVERSE DIRECTION

LONGITUDINAL DIRECTION

TABLE 1F RELATIVE INTENSITY vs POSITION MATRIX

- NON SPECULAR REFLECTOR ($\sigma = 2^0$)
- INDUCED DISTORTION (TWIST = 4^0)

7	6	7	7	7	7	8	8	8	8	8
6	7	6	7	7	8	7	7	8	8	8
7	7	7	8	8	8	7	8	8	9	9
8	9	10	8	10	11	11	12	12	13	13
11	12	13	13	13	13	12	12	10	10	10
12	12	10	9	9	8	8	8	8	8	8
8	8	8	8	7	8	8	8	7	8	7
7	6	7	7	7	6	7	8	7	7	6
7	7	7	7	8	8	7	6	4	3	3
7	8	10	8	5	3	2	2	3	2	2

TRANSVERSE DIRECTION

LONGITUDINAL DIRECTION

TABLE 1G RELATIVE INTENSITY vs POSITION MATRIX

- NON SPECULAR REFLECTOR ($\sigma = 4^0$)
- INDUCED DISTORTION (TWIST = 4^0)

6	6	6	6	6	6	7	7	7	7	7
6	6	7	6	7	7	7	7	7	7	7
8	7	8	8	8	8	8	8	8	8	8
7	7	7	6	7	7	7	6	7	6	6
6	6	7	6	6	6	7	6	6	6	6
6	7	6	6	6	6	7	7	7	8	7
7	8	8	8	8	8	7	8	8	7	6
7	8	7	7	6	6	6	6	6	6	5
6	6	5	6	6	5	6	6	6	5	6
6	6	6	6	5	7	6	6	6	6	6

TRANSVERSE DIRECTION

LONGITUDINAL DIRECTION

towards the upper edge and become very intense at the extreme edge of the 4° case. The effect of non-specularity in the mirror on the undistorted case (twist=0) is shown in Table 1 d, and e for $\sigma = 2°$ and $\sigma = 4°$. The intensity distributions become smooth in the former case and essentially flat in the latter. Finally, the effect of non-specular reflectors under extreme twist is shown in Table 1 f and g, where again this technique dramatically reduces or effectively eliminates non-uniformities.

3) Calculations of the distributions under variable concentration. Activation of the variable concentration configurations by tilting the mirrors to close the aperture ratio does change the distribution from those produced by the fully deployed CPC. However, as could be expected, ray traces show that the non-specular reflector technique is similarly effective in smoothing these distributions. For example, the distributions for normal incidence ($\theta = 0°$) on nominal 4.67 x CPC are shown in Figure 19 for two intermediate concentrations of 3.5 x (dashed) and 2.5 x (solid line). For the worst case specular reflector ($\sigma = 0°$) it can be seen that the peaks move away from the center and spread farther apart as the concentration is lowered. The non-specular reflectors smooth ($\sigma = 2°$) or eliminate ($\sigma = 4°$) peaks as shown.

4) Calculation of the effects of variation of mirror spacing (i.e. blanket width) without redesign of concentration profile shape. Figures 20a and 20b show the partially smoothed ($\sigma = 2°$) distribution for a nominal 4.0m exit aperture, 4.67 x, $\pm$ 5° CPC, if the exit apertures were 4.5 meters and 3.5 meters respectively. In the former case, although all the light in the concentrator strikes the absorber, the absorber plane is too wide so that there is a drop-off at the edges

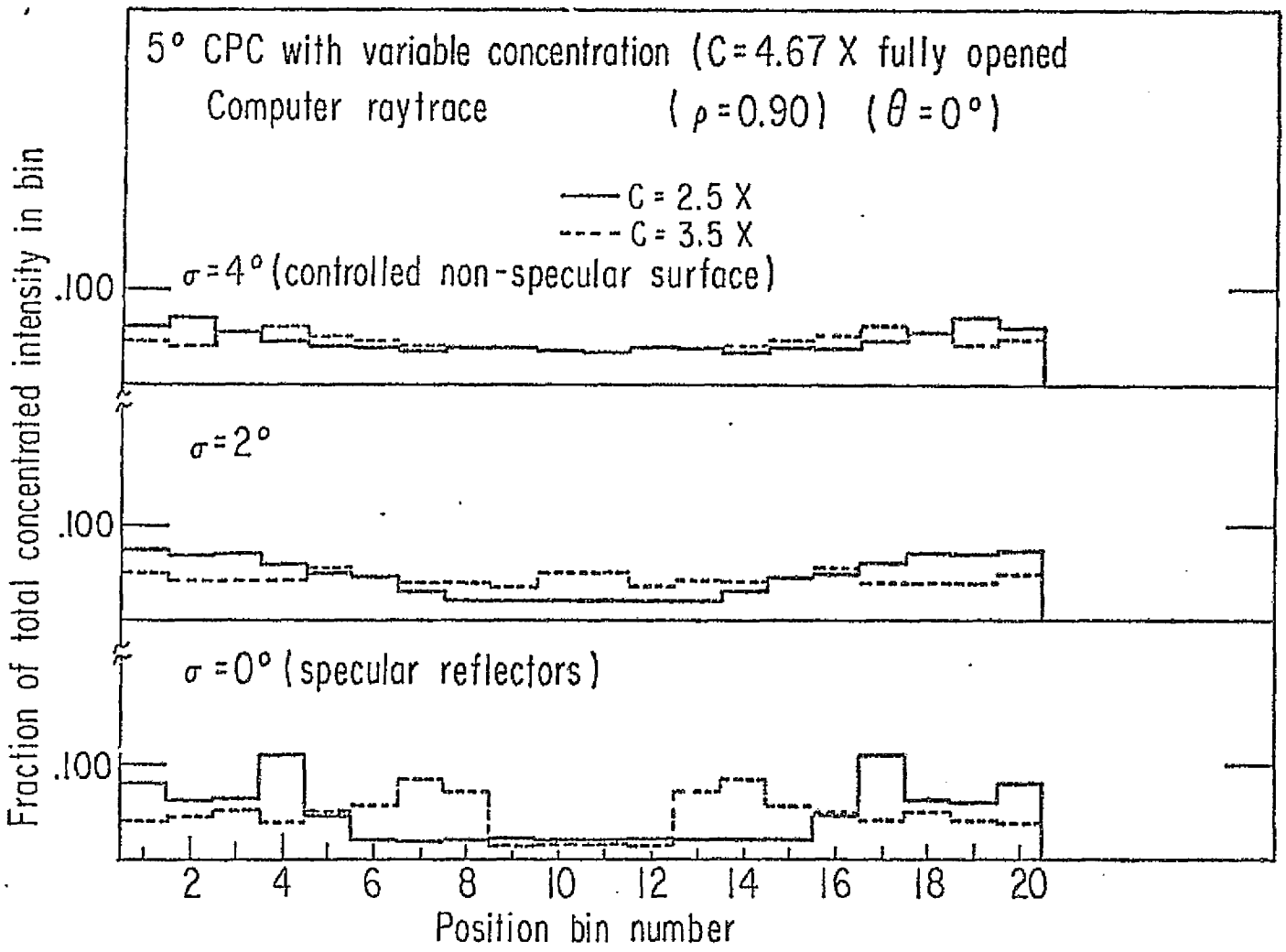

FIGURE 19 CALCULATED INTENSITY DISTRIBUTIONS UNDER VARYING CONCENTRATION

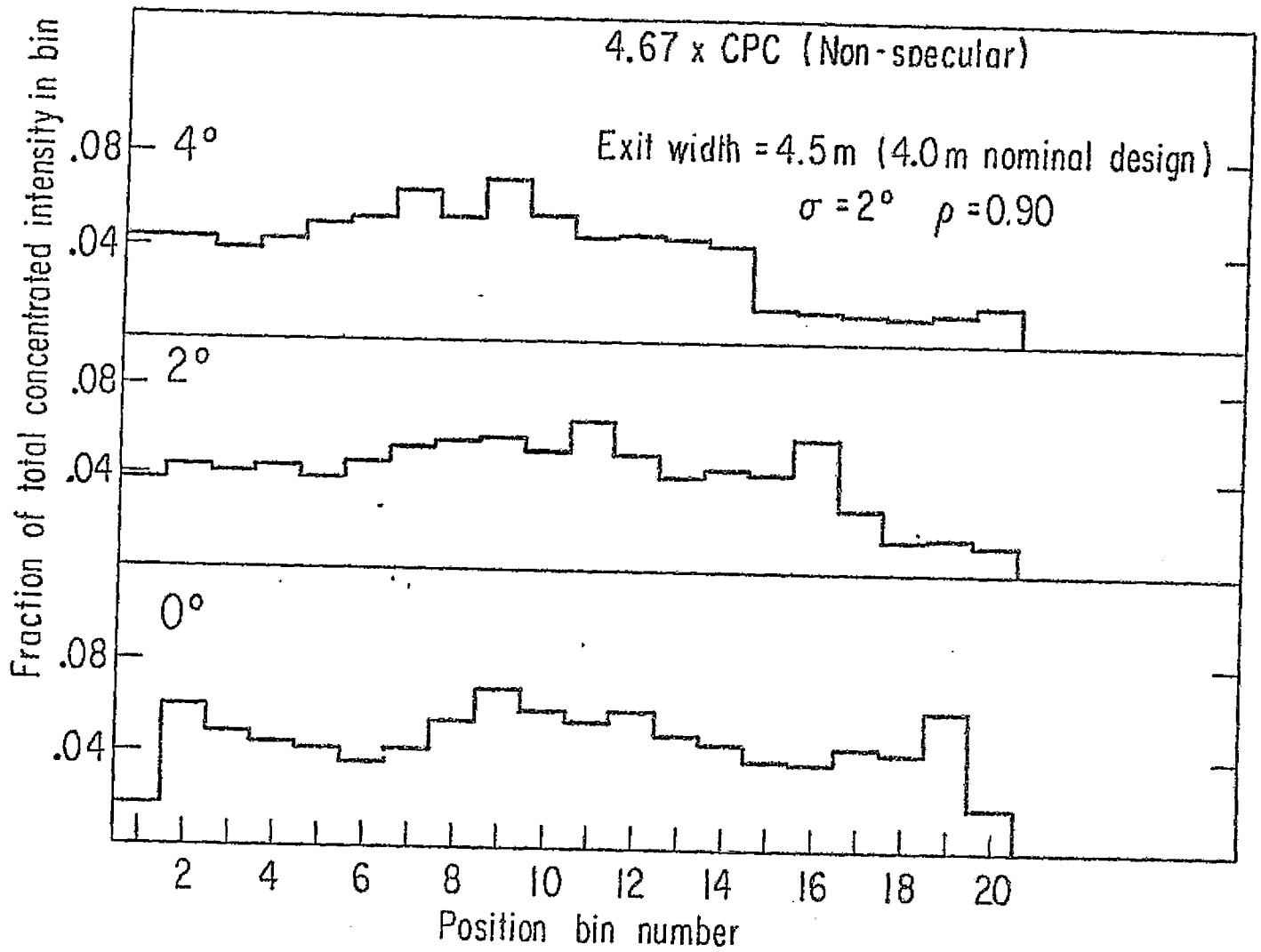

FIGURE 20A

ASPECT TOLERANCE: CALCULATED INTENSITY DISTRIBUTION WITH OVERSIZED ABSORBER

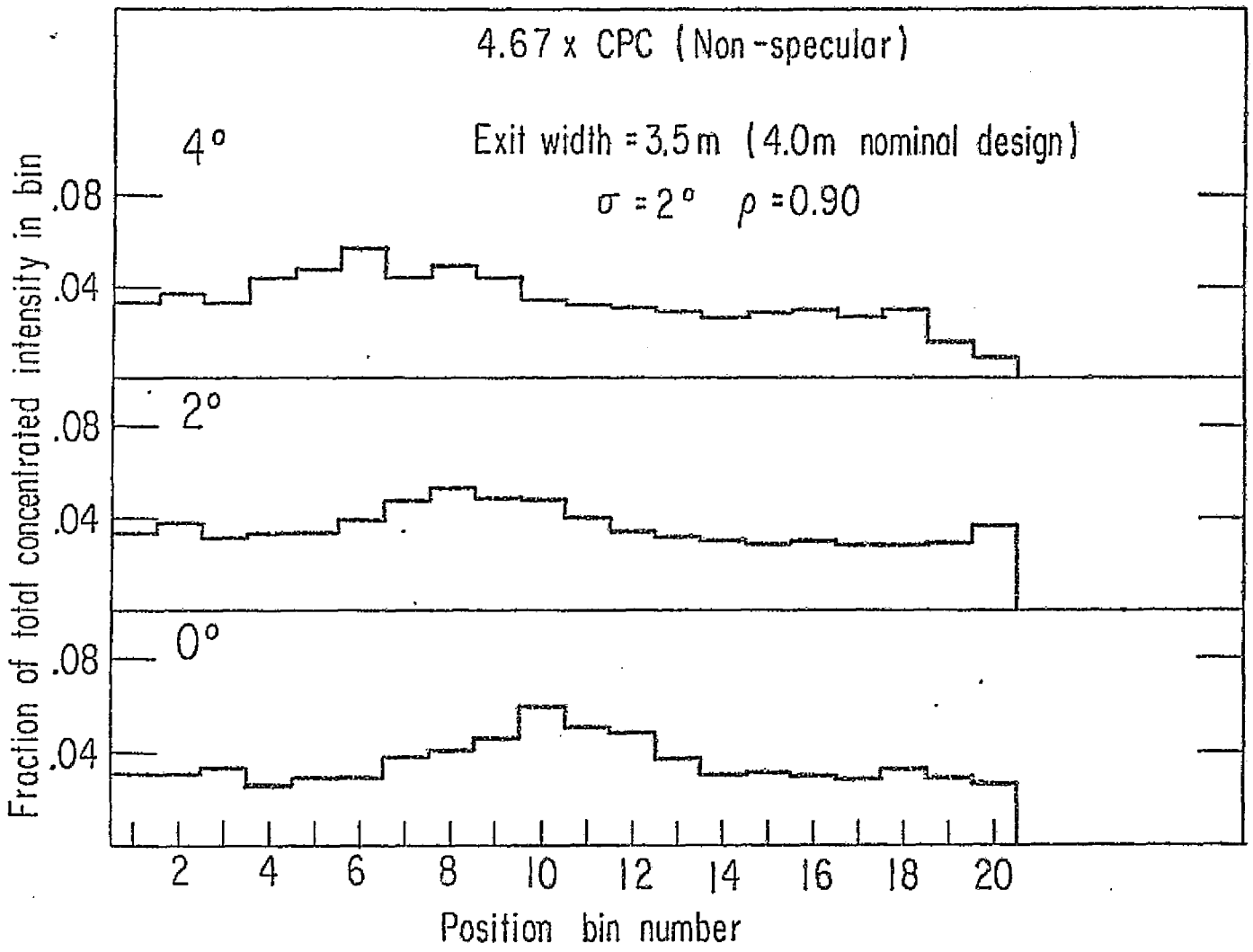

FIGURE 20B ASPECT TOLERANCE: INTENSITY DISTRIBUTION ON UNDERSIZED ABSORBER

where only direct radiation reaches. In the latter case some light is lost since the outer edges of the nominal distribution now strikes mirrors and are reflected back out. Thus the collection efficiency (fractional throughout) decreases as the exit width is decreased below nominal as shown in Figure 21a. The geometrical concentration ratio, however, is increasing at the same time so that the net concentration (product of efficiency times geometric concentration ratio) is very insensitive to this parameter as shown in Figure 21b.

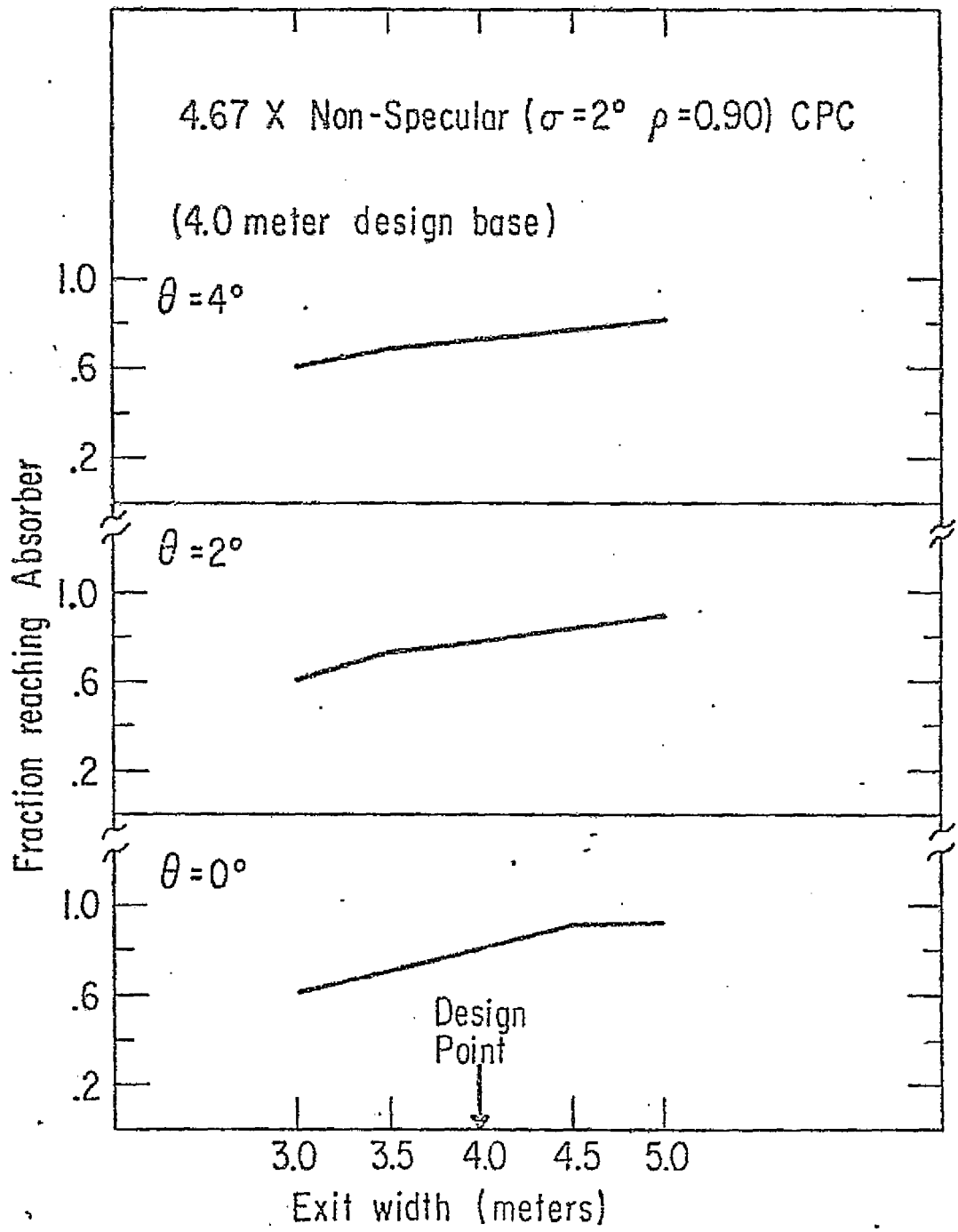

FIGURE 21A ASPECT TOLERANCE: COLLECTOR ACCEPTANCE WITH VARYING EXIT WIDTH

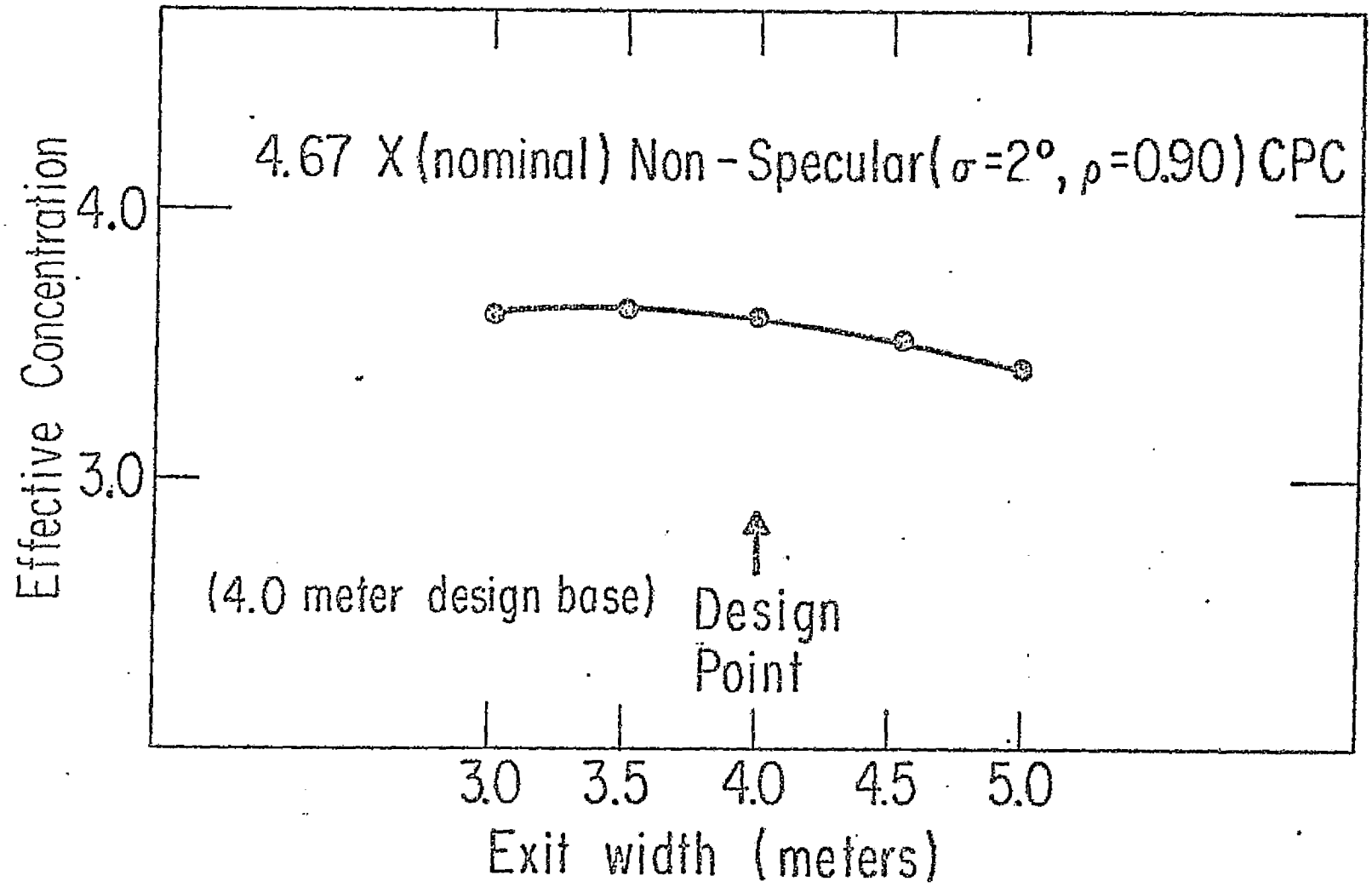

FIGURE 21B ASPECT TOLERANCE: EFFECTIVE CONCENTRATION OF COLLECTOR WITH VARYING EXIT WIDTH

V. Survey of Alternate Optical Approaches

The fundamental advantages of CPC's are the ability to achieve intermediate values of geometric concentration ratio (1.5 x - 10 x) with wide viewing angles resulting in relaxed tolerances on pointing accuracies, mirror surface slope errors, system alignments, and positioning errors etc. Furthermore, for concentration ≤ 5 x, this can be done with height to aperture ratios ~ 1. The question arises as to how these advantages compare with those of other systems designed for the same basic objectives. Imaging systems, which use focussing optics, generally are having small mirror areas for given concentration ratio but require high pointing accuracy and mirror accuracy. A brief analysis of the features of three types of non-imaging concentrators was carried out and the results are summarized in what follows. The three different designs considered were: a) the familiar striaght sided vee-trough; b) curved side wall trough reflectors designed to distribute the radiation uniformly on the absorber blanket for one particular incidence angle (here $\theta = 0°$) referred to as uniform distribution concentrators (UDC's); and c) two stage non-imaging concentrators capable of concentrations in the range 5 x - 10 x.

A. Vee-trough Concentrators

The obvious advantage of such an approach is simplicity, and for low concentrations (geometrical ratios ≤ 2) such designs may be preferred. The disadvantages are that for geometrical concentrations $\geq$ 2.5, both the height-to-aperture ratio and the average number of reflections (hence optical losses) increase rapidly. An example of

a vee-trough with geometrical concentration of 4.67, the same as the baseline CPC compared with it, is shown in Figure 22. Furthermore, it should be noted that this vee-trough has an angular response which varies strongly with angle. A detailed study of the behavior of a wide variety of vee-troughs and their comparison with CPC's has been carried out recently (Ref. 6). The Table summarizing the major results is reproduced here as Table 2. The angle γ corresponds to θ in our notation. The vee-trough is designed for an almost flat angular response up to $\theta = \gamma_s$ (i.e. γ_s corresponds to our θ_c) with the light at $\gamma = \gamma_s$ undergoing a maximum of N reflections. Note in particular that for net concentrations (after optical losses) $C_{net} \geq 2$ the vee-trough has lower concentration and larger side to base ratio than the CPC with the same C_{net}. Vee-troughs with $\gamma_s > 0$ have larger side to base ratios than $\gamma_s = 0$ vee-troughs with the same C_{net}.

B. The Uniform Distribution Concentrator (UDC).

In general, if one restricts incident radiation to parallel light at a particular angle (say $\theta = 0^{\circ}$) one can construct a concentrator mirror shape which will distribute the light uniformly on the absorber. In fact, there are an infinite number of such solutions but only a few of reasonable practical interest. An analysis of several of these configurations was carried out during Phase II and the major conclusions are summarized here. The advantage of such a solution is, of course, the desired uniformity at $\theta = 0$. The disadvantages are:

1) that in general, such solutions have larger height to aperture ratios than CPC's of the same concentration. See, for example, the comparison in Figure 23 of the smallest 4 x UDC with a 4 x CPC. The UDC is 20% taller.

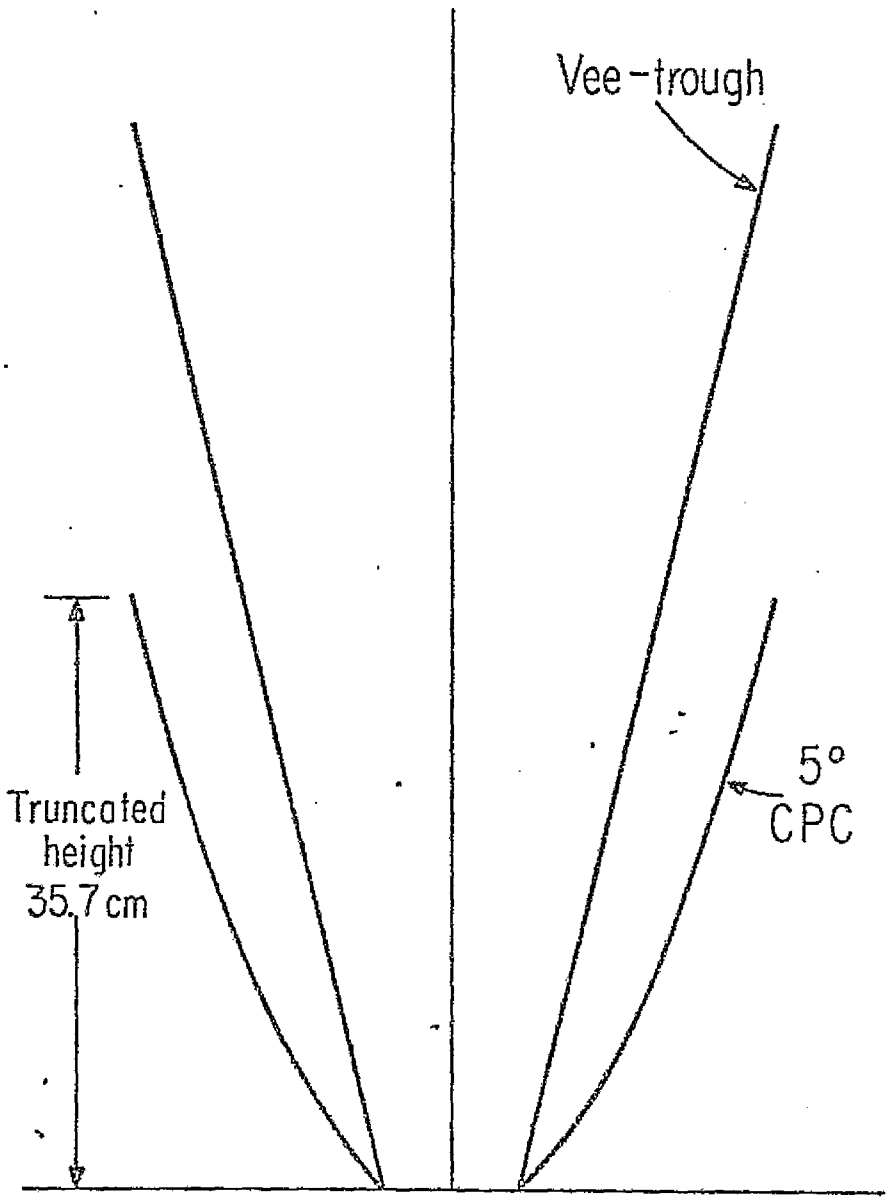

FIGURE 22 COMPARISON OF PROFILES OF TWO 4.67 X CONCENTRATORS (CPC AND VEE-TROUGH)

TABLE 2 SIDE-TO-BASE RATIO REQUIRED FOR A GIVEN CONCENTRATION FACTOR, FLAT-SIDED TROUGH, AND THE TRUNCATED CPC*

N-VALUE FOR TROUGH	FLAT-SIDED TROUGH			TRUNCATED CPC † $\gamma_s \equiv \theta = 10^0$	
	CONC. FACTOR, C		SIDE TO BASE RATIO L/D_0	CONC. FACTOR, C	SIDE TO BASE RATIO L/D_0
	$\gamma_s = 0$	$\gamma = 10^0$			
N = 1, ρ = 1	2.5	2.0	2	2.5	1.25
N = 1, ρ = 0.8	2.2	1.8	2	2.5	1.6
N = 2, ρ = 1	3.5	2.5	4.5	3.5	3.5
N = 2, ρ = 1	4	2.7	6.6	4	4.8
N = 2, ρ = 0.8	3	2.2	5	3	3.5
N = 3, ρ = 1	4.5	2.75	8	4.5	6.5
N = 3, ρ = 0.8	3.5	2.3	8	3.5	4.7

*TAKEN FROM BURKHARD, STROBEL, AND BURKARD, "FLAT-SIDED RECTILINAR TROUGH AS A SOLAR CONCENTRATOR: AN ANALYTICAL STUDY", APPLIED OPTICS, 15 JUNE 1978, VOL. 17.

†NOTE THAT FOR CONCENTRATIONS ≥ 2 AND COMPARABLE DESIGN CRITERIA, THE VEE-TROUGH HAS LOWER CONCENTRATION AND LARGER SIDE TO BASE RATIO

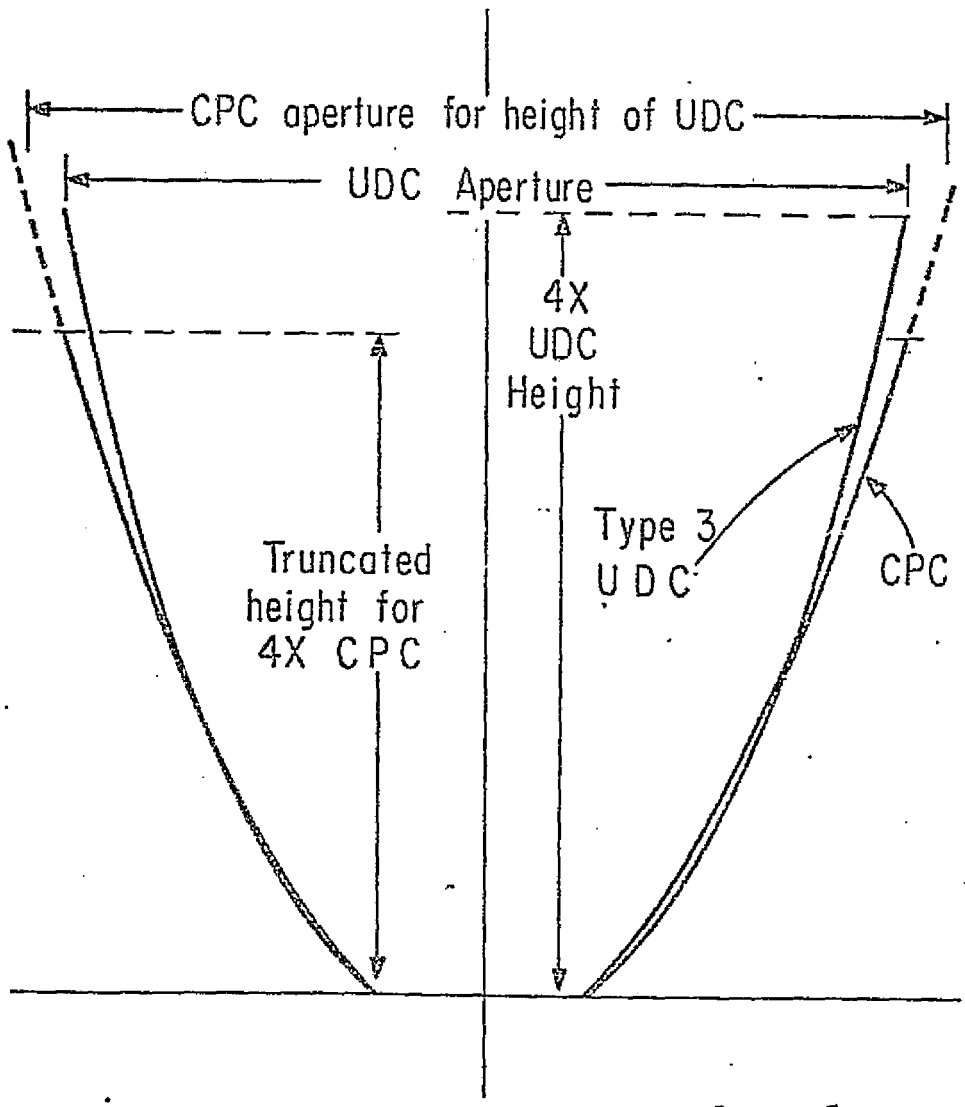

FIGURE 23 REFLECTOR PROFILE CURVES FOR CPC ($\theta_c = \pm 5°$)
AND BEST 4X UNIFORM DISTRIBUTION CONCENTRATOR

2) The uniformity is attained only at precisely one incidence angle. As soon as $\theta \neq 0$ by even 1°, peaks appear in the distribution as shown by the solid line in Figure 27, which is based on a computer ray trace. If, then, one introduces a non-specular reflector as is proposed for the CPC one smooths the peaks but is left with a distribution virtually the same as that from a CPC, as is to be expected since Figure 23 shows that the two solutions are very similar. Finally, it should be noted that the angular response of the UDC is somewhat narrower and more variable than that of the CPC .

C. Two Stage Non-Imaging Concentrator

If one desires geometrical concentrations in the range 5 X - 10 X. the combination of a focussing primary and a non-imaging secondary can achieve this with a large acceptance view angle $\geq \pm 5°$ while still maintaining reasonable overall dimensions. It also has some advantages over a specular single stage CPC in that the rays reflected from the primary "fill" a larger portion of the acceptance of the secondary, and thus reduce somewhat the intensity variation even at these higher concentrations. The major questionable feature of such an approach is the design of a configuration that can be implemented in space. Both symmetric and asymmetric configurations are possible. A conceptual drawing of a possible symmetric configuration is shown in Figure 25 while a line drawing of the profile for one particular asymmetric design is shown in Figure 26. This latter design is the basis for a series of preliminary computer ray trace studies carried out to investigate the basic optical properties of the two stage approach

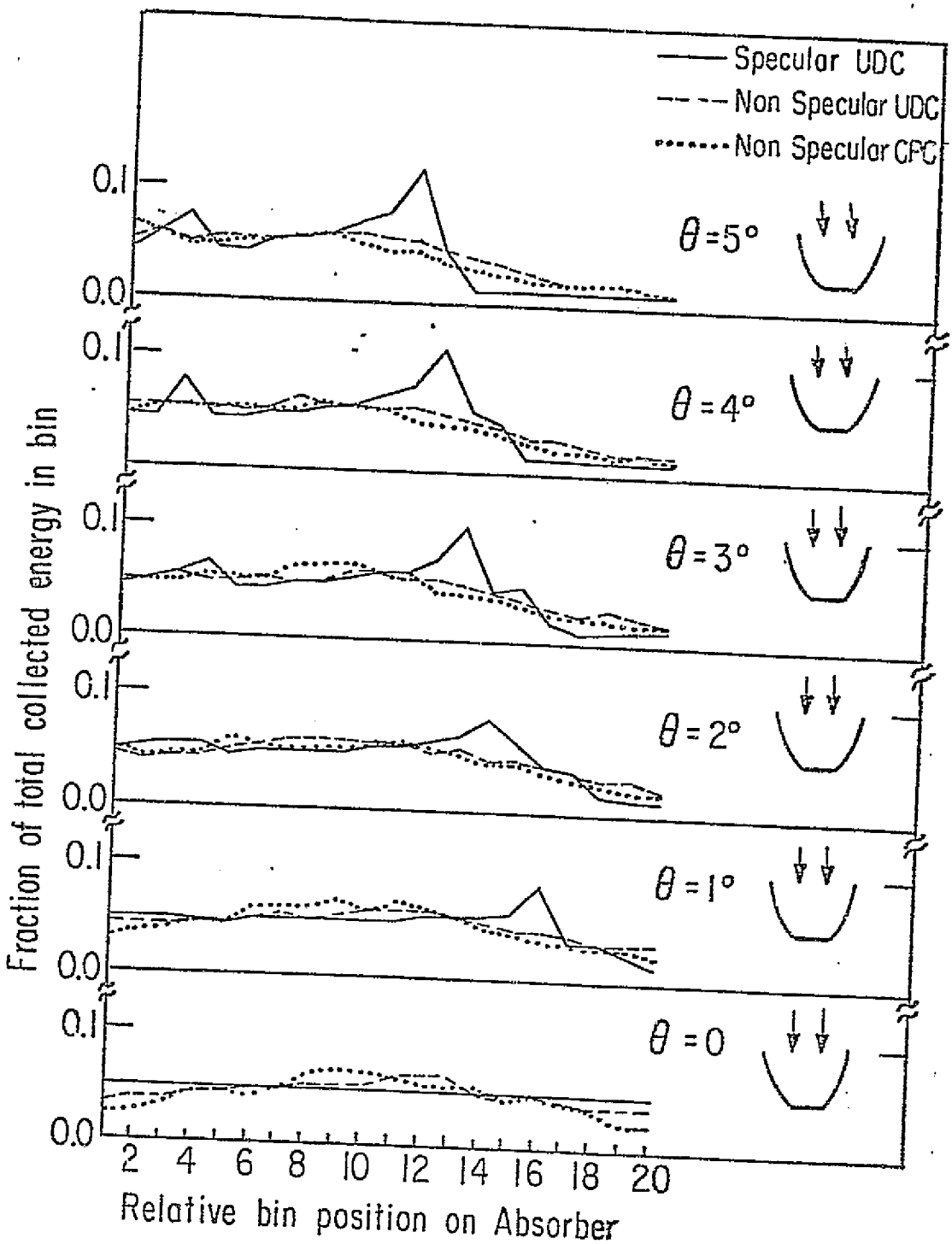

FIGURE 24 RELATIVE INTENSITY DISTRIBUTION ON ABSORBER FOR THREE CONCENTRATOR DESIGNS

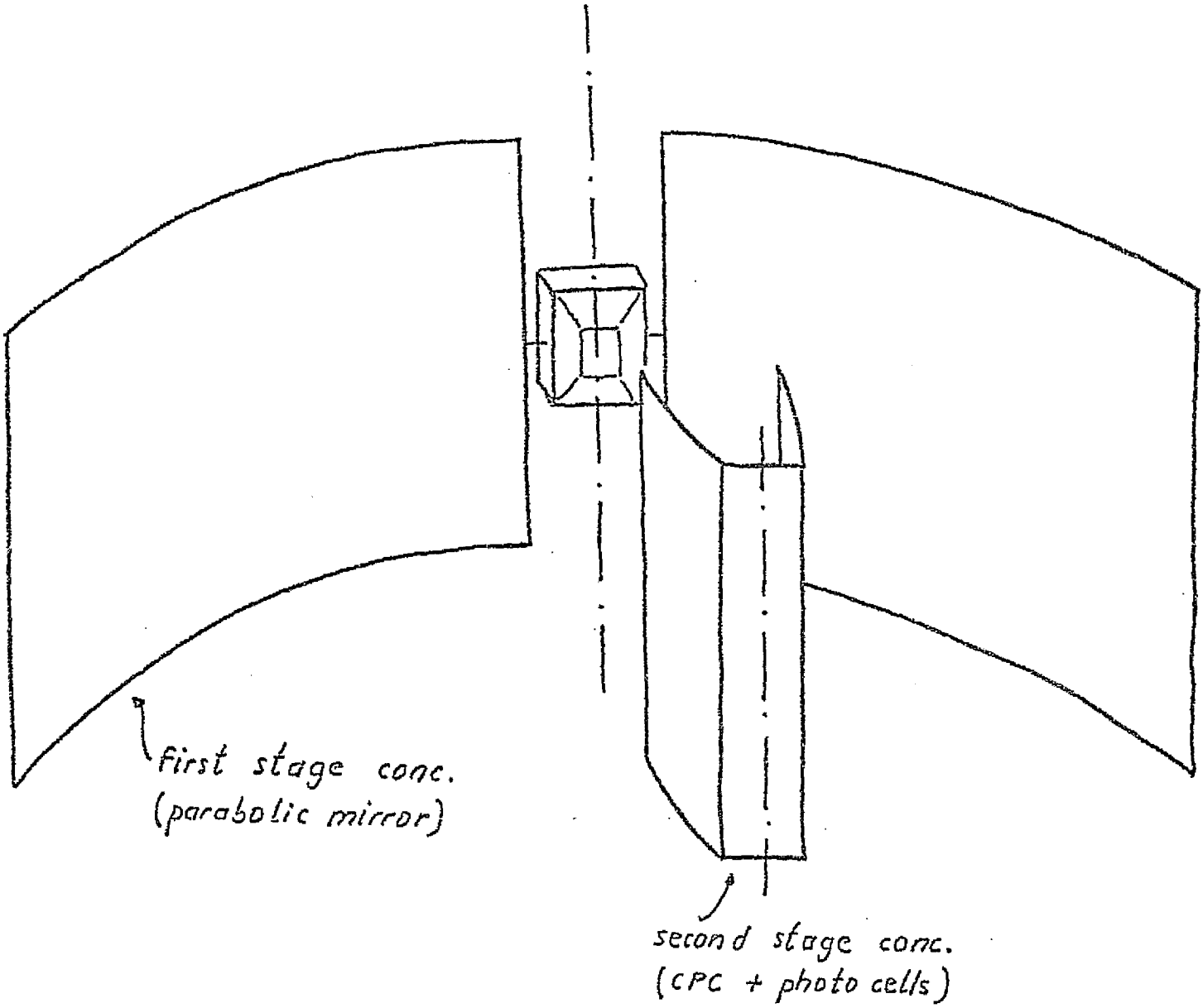

FIGURE 25 10 X TWO STAGE CONCEPT

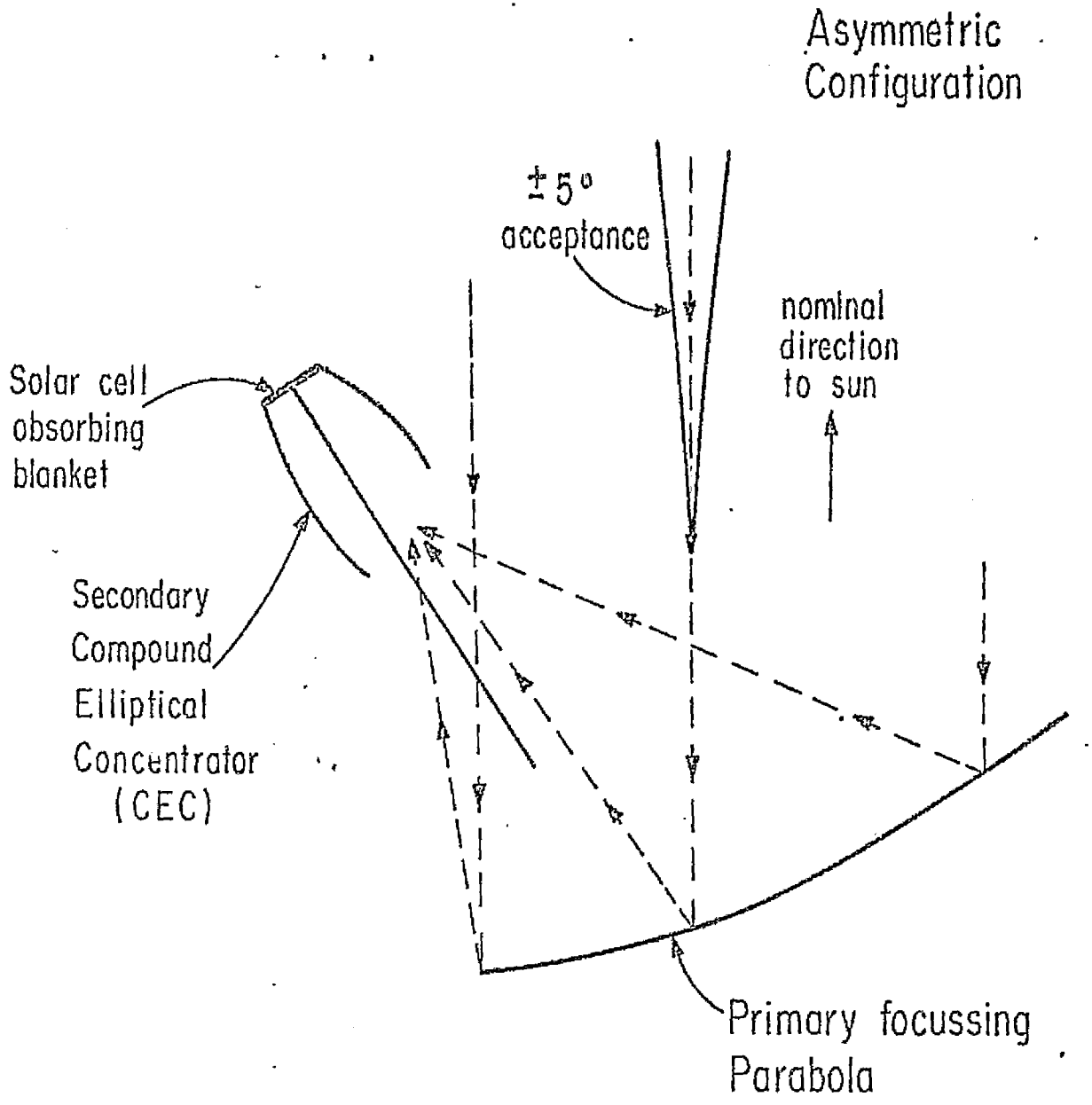

FIGURE 26 ALTERNATE CONCEPT DESIGN FOR NON IMAGING "IDEAL" SPACE CONCENTRATOR (C UP TO 10 X) : ASYMETRIC CONFIGURATION

as well as for an actual model built and tested at the University of Chicago. Calculated intensity distributions on the absorber for incidence angles of 0°, ± 2", and ± 4° are shown in Fig. 27a where specular reflectors have been used in both the primary and secondary reflectors and in Fig. 27b where a controlled non-specularity of $\sigma = 2°$ has been incorporated into the secondary while the primary remains specular. Note first that the distribution is quite smooth even with specular reflectors for $|\theta| \leq 2°$. At the more extreme angles of ± 4°, peaks appear in the distribution ~ 5 times the average intensity which are substantially reduced although not eliminated completely by a second stage with $\sigma = 2°$. The fact that some variations remain in the latter case can be qualitatively understood in terms of the relative magnitude of the scattering parameter (2°) compared to the acceptance angle of the second stage (~ ± 20°).

Some very recent studies have indicated that a more effective approach may be to introduce a small scattering ($\sigma \leq 1°$) into the primary reflector and use a specular second stage. The results of a ray tracing such a design with $\sigma = .5°$ and $\sigma = 1°$ are shown in Fig. 27c. In addition, results with scattering added to both stages are shown in Fig. 27d. Fig. 28 shows the angular response of the two stage under these three conditions.

Finally, to demonstrate experimentally the potential of the two-stage - non-imaging approach, a test model was built, conceptually similar to the design in Fig. 26. The test model, however, had an acceptance angle of ± 6° and a geometric concentration of 7.9. The measured intensity distribution for near normal incidence attained by this design <u>with specular reflectors</u> is plotted in Fig. 29. Even with no attempt to smooth irregularities the variations are ~ ± 20%. The optical efficiency is very high (88 ± 6%) corresponding to a <u>net</u> effective gain of 7.0 ± 0.5 since there are no scattering losses. Highly reflecting Sheldahl silver foil ($\rho \cong 0.95$) second stage reflectors were used in this test. The primary reflector was anodized aluminum sheet.

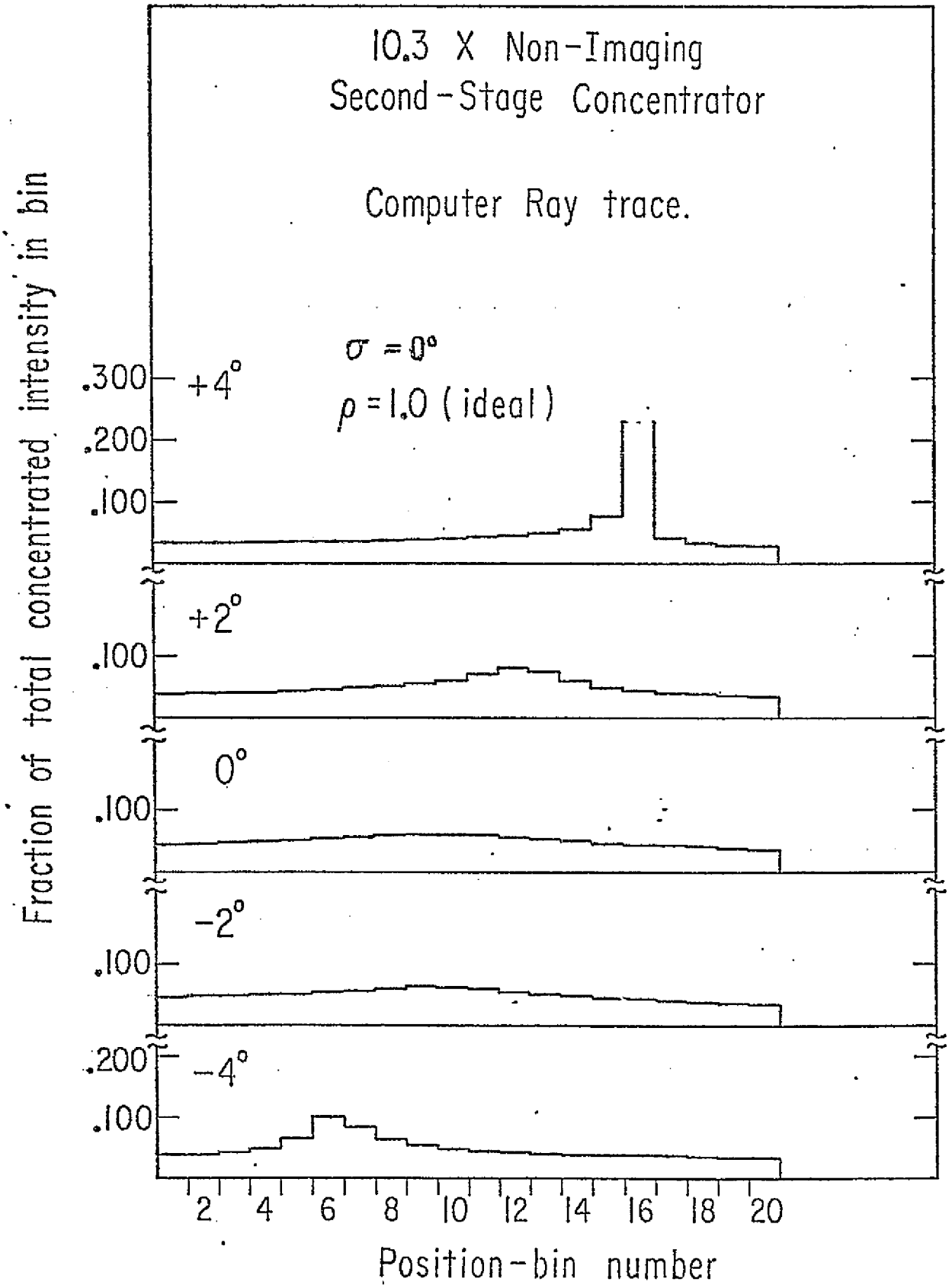

FIGURE 27A LIGHT DISTRIBUTION ACROSS EXIT OF SECOND-STAGE CONCENTRATOR: SPECULAR REFLECTORS

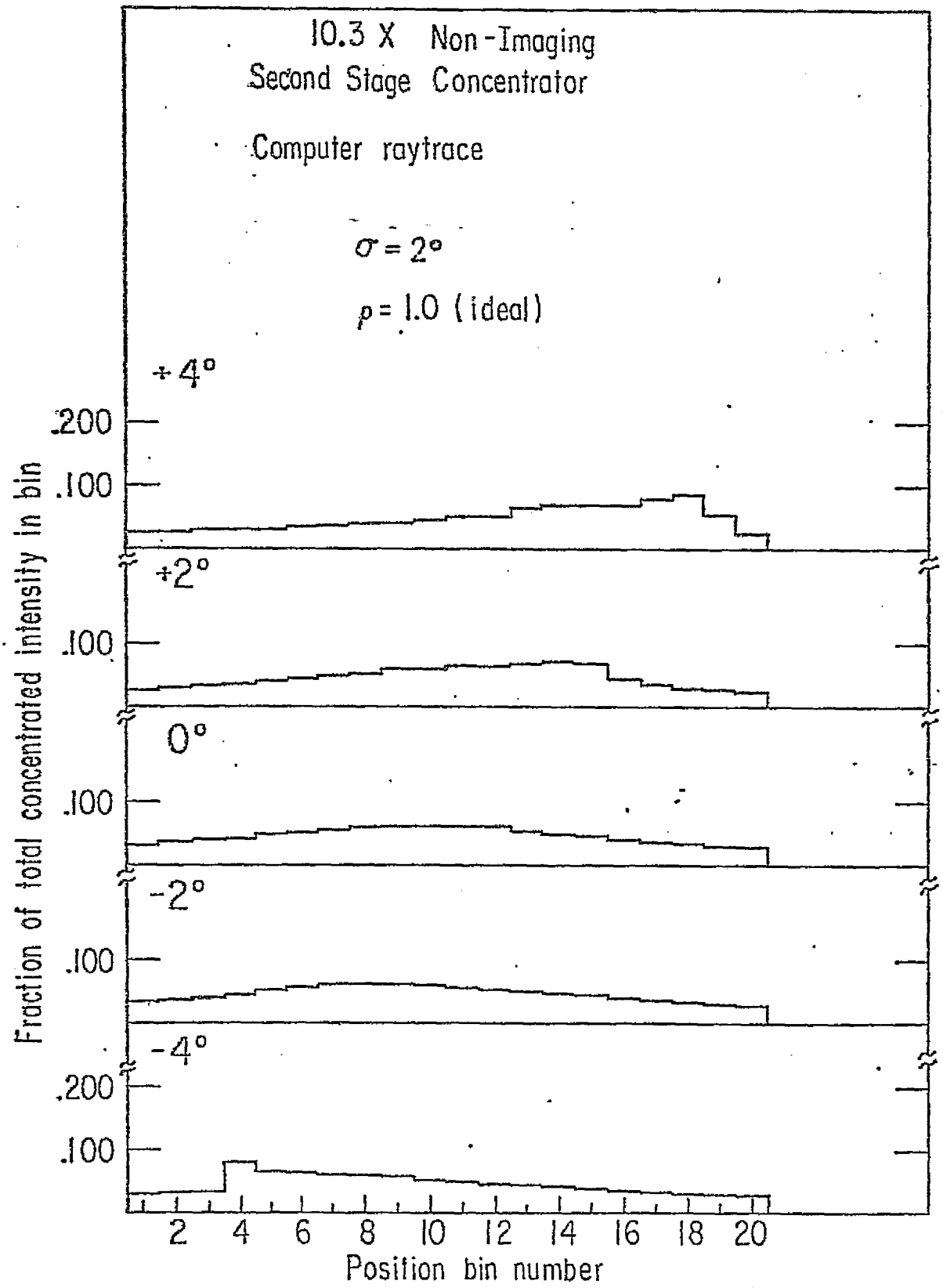

FIGURE 27B CALCULATED LIGHT DISTRIBUTION ACROSS EXIT OF SECOND-STAGE CONCENTRATOR: SPECULAR PRIMARY, NON-SPECULAR SECONDARY

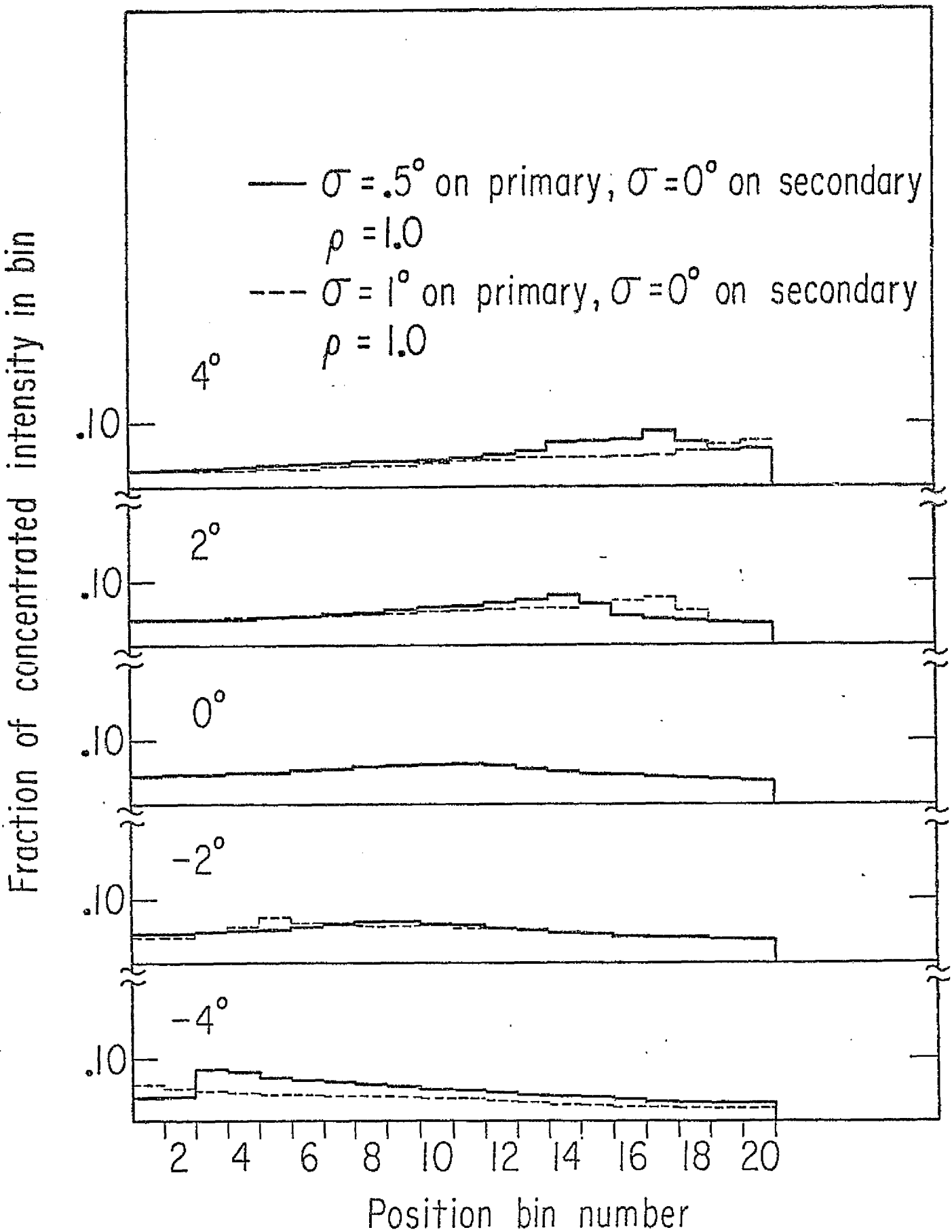

FIGURE 27c CALCULATED INTENSITY DISTRIBUTION ACROSS EXIT OF 10.3 X SECOND STAGE CONCENTRATOR; NON-SPECULAR PRIMARY, SPECULAR SECONDARY

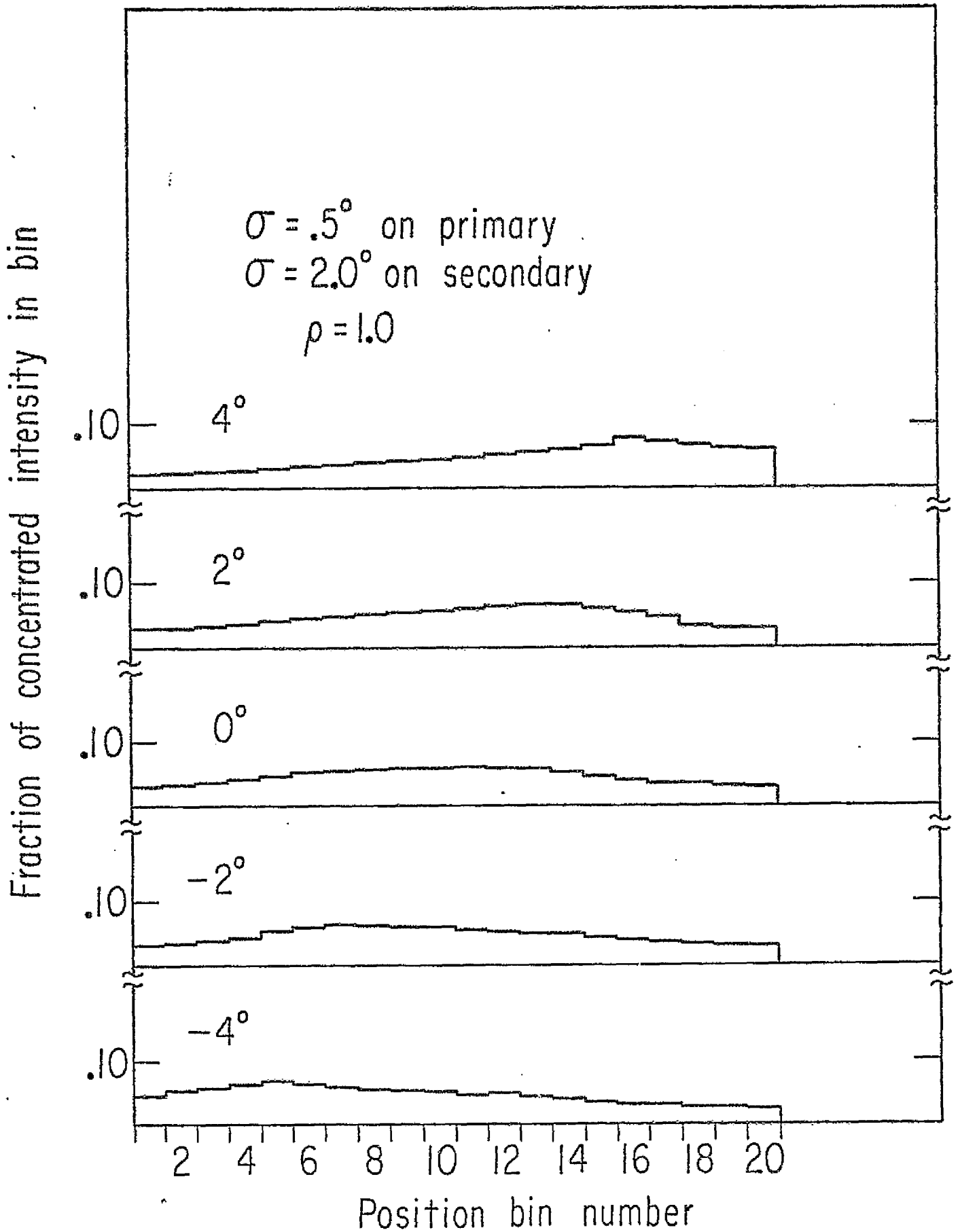

FIGURE 27D CALCULATED INTENSITY DISTRIBUTION ACROSS EXIT OF 10.3 X SECOND-STAGE CONCENTRATOR: NON-SPECULAR PRIMARY AND SECONDARY

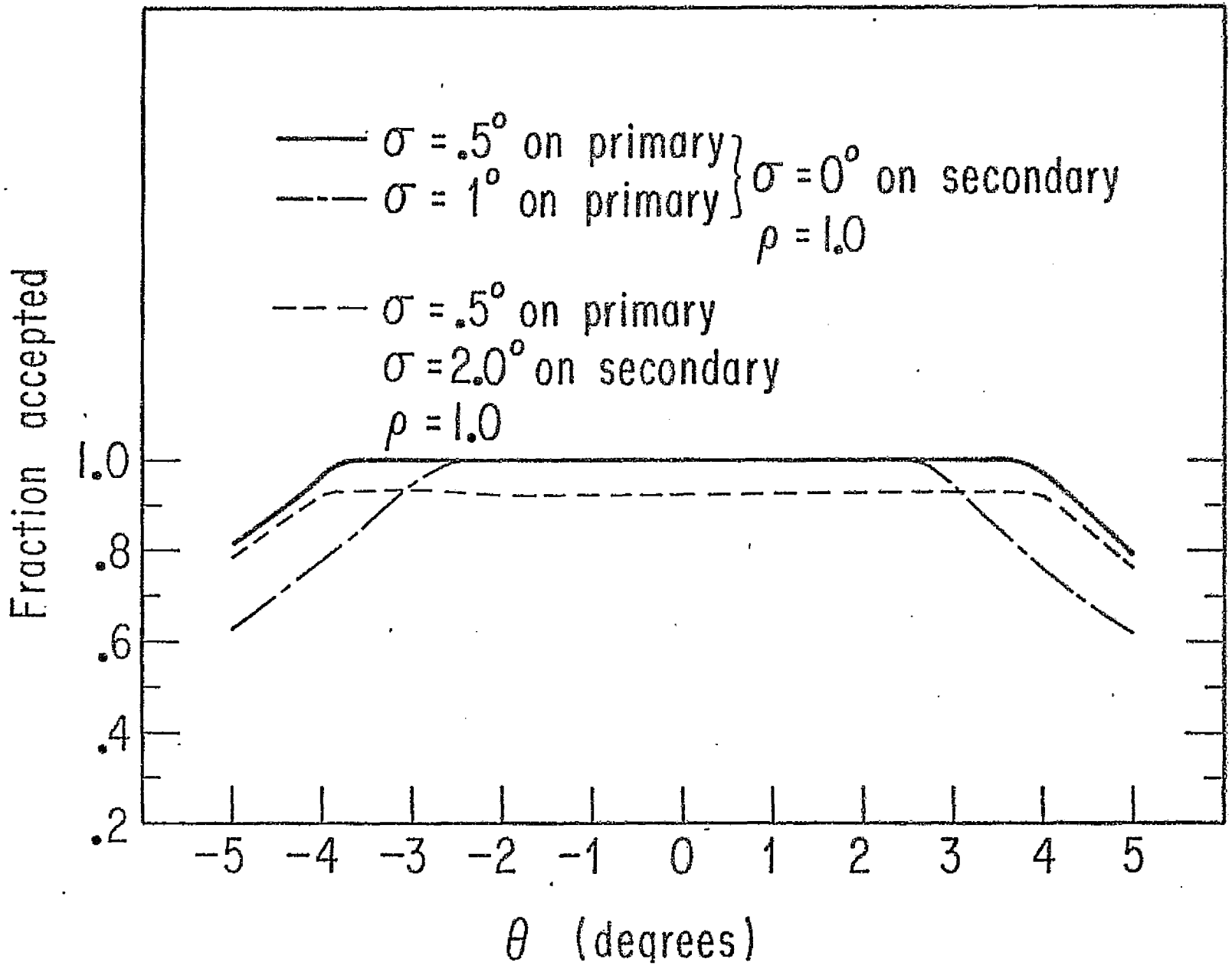

FIGURE 28 CALCULATED ANGULAR RESPONSE OF 10.3 X TWO-STAGE CONCENTRATOR WITH VARIOUS REFLECTOR SURFACES

Angular Acceptance : $\theta_{max} = \pm 6^\circ$
Geometric Concentration : $C = 7.9$
Measured Gain : $C = 7 \pm .5$

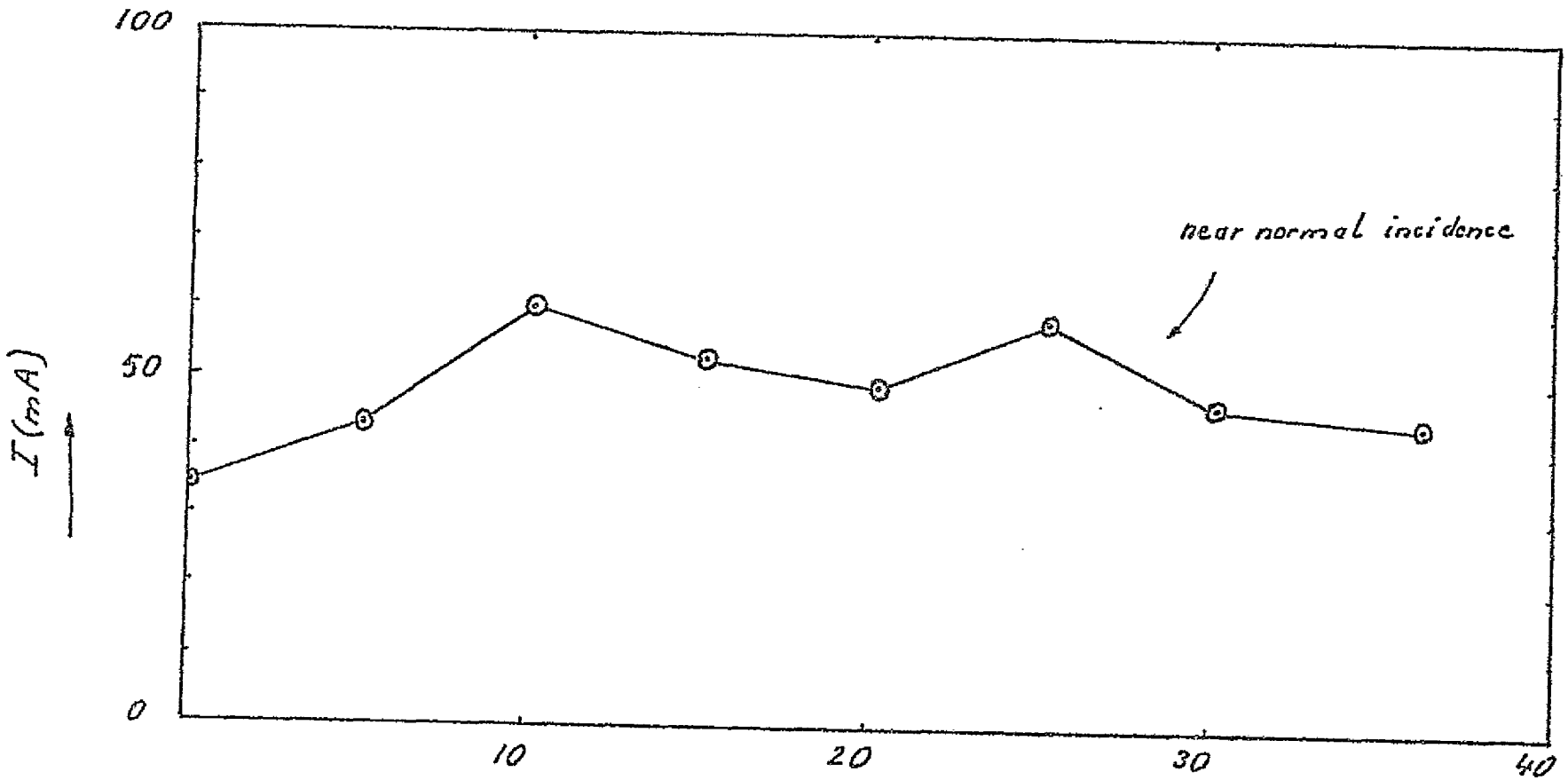

FIGURE 29 MEASURED INTENSITY DISTRIBUTION ACROSS EXIT OF SECOND STAGE CONCENTRATOR

VI. Summary and Recommendations

The major findings resulting from Phase II of the contract effort are summarized below:

1) Compound Parabolic Concentrators (CPC's) provide the widest possible view angle and maximum tolerance for mirror surface, slope and alignment errors for application in a large concentrator in space.

2) The design lends itself readily to activating variable geometrical concentration.

3) Tests at General Electric Space division confirmed the presence of predicted intensity variations of an 80 cell modular array under varying concentration ratios from 1.75 - 4.67.

4) Further tests at the University of Chicago under terrestrial sunshine show that the introduction of a controlled degree of non-specularity into the concentrator mirror surface provides a very effective method for reducing intenstiy variations resulting from more severe conditions and furthermore demonstrated the extreme reliability of analytical predictions based on Monte Carlo computer ray trace technique.

5) Extensive computer ray trace of the baseline 4.67 X, $\pm$ 5° variable concentration CPC shows that this is a viable preliminary design from the optical point of view for a cometary mission.

6) Ray trace and experimental studies of two-stage non-imaging systems may be advantages if geometrical concentrations > 5 are desired.

Based on work to date, establishing feasibility of the basic approach, a number of open areas remain for further design study before a space-

worthy operating design could be finalized.

Therefore, in the continuing effort to develop a practical concentrator-array system it is recommended that further work to refine and improve the concept be carried out specifically in the following areas:

1) Analyze the trade-offs between cell blanket performance, degree of non-uniformity and associated optical loss directed towards determining the optimum combined concentrator-cell blanket array configuration.

2) Search for a material suitable to:

   a) provide a light weight substrate for metallized reflective coating;

   b) accept and hold a surface texturing (to improve the required degree of non-specularity) in a manner similar to Mylar;

   c) survive the space environment.

3) Determine the best method for accurately and reproduceably producing large areas of suitable foil with the desired values of non-specularity parameters.

4) Study further the applicability of the two stage design for higher concentration.

List of References

1) JPL Contract 954 563 (Phase I), Final Report.

2) Hinterberger H. and R. Winston, Rev. Sci. Instrum. 37, 1094 (1966).

3) Baranov, V.K., Geliotekhnika 2, 11 (1966).

4) Ploke, M., Optik 25, 31 (1967).

5) Rabl, A., Solar Energy, 18, 93 (1976).

6) Burkhard, D., G. Strobel, D. Burkhard, Applied Optics, 17, 1870 (1978).